TECHNICAL MEMORANDUM Copy No.___

ESL-TM-345

A THREE-STATE CLUTCH SERVOMECHANISM FOR AN UNDERWATER CONTROL SURFACE

by

Carl R. Tegnelia

May, 1968

Contract No. NOw-66-0178d

The preparation and publication of this report, including the research on which it is based, was sponsored by the Naval Ordnance Systems Command, Department of the Navy, under Contract No. NOw-66-0178d, M.I.T. DSR Project No. 76094. This technical memorandum is published for technical information only and does not represent recommendations or conclusions by the sponsoring agency. Reproduction in whole or in part is permitted for any purpose of the United States Government.

Approved by: George C. Newton, Jr.
George C. Newton, Jr.
Associate Director

Electronic Systems Laboratory
Department of Electrical Engineering
Massachusetts Institute of Technology
Cambridge, Massachusetts 02139

ABSTRACT

The problem of designing a three clutch servomechanism for positioning the control surfaces of a small underwater vehicle is considered. Clutches with on-off control are employed to satisfy demands on efficiency, reliability, and weight and also minimize clutch heating. Two clutches in the system drive the load clockwise and counterclockwise while the third clutch brakes the load to ground on the vehicle body. The drive clutches are connected to the load shaft through a spring and a gear train. The spring reduces drive clutch slippage losses but complicates the control system design.

A partial mathematical analysis of the system is performed, but final conclusions are based on analog simulation results. Best performance is achieved with a coupled two-loop control system; one loop controls the actuation of the drive clutches and the other the actuation of the brake clutch and drive clutch actuation inhibit. The optimum form of this system has a rise time of 20 ms. for a 3.5 degree step input and a steady-state error less than 7 minutes. For a sinusoidal input with a magnitude of 3.5 degrees, the response is flat out to 7 Hz and the system bandwidth is 27 Hz. For a switching delay of 1.5 ms, bandwidth is reduced but other performance measures are not significantly affected.

ACKNOWLEDGMENT

The material presented in this technical memorandum is based on a thesis submitted in partial fulfillment of the requirements for the degree of Master of Science and Electrical Engineer at the Massachusetts Institute of Technology in May, 1968.

This work was supported by the Naval Ordnance Systems Command, Department of the Navy, under Contract No. NOw-66-0178d, M. I. T. DSR Project No. 76094.

The author wishes to thank Prof. George C. Newton for undertaking the supervision of this thesis and for contributing valuable criticisms. Sincere thanks are also due Dr. Richard W. Bush, whose many suggestions were the guiding influence in this work.

CONTENTS

CONTENTS (Contd.)

LIST OF FIGURES

LIST OF FIGURES (Contd.)

CHAPTER I

INTRODUCTION

1a. Statement of the Problem

In the design of a clutch servomechanism for a small underwater control surface, it is desirable that the servo be small, highly efficient, reliable, and inexpensive. In an environment in which mechanical power is readily available, a clutch system operating in a switching mode is a logical choice to satisfy these requirements. One such system using a two-state clutch with bang-bang* control was described in a thesis by Robert Cheney,[1] and the design work for realizing the system was done by A. H. Firodia.[2] Although this research produced satisfactory results on the whole, the resulting system exhibits steady state oscillations because the bang-bang servo is unable to provide for quiescent states. Such oscillations cause unnecessary wear and heating and may result in considerable hydrodynamic noise.[1] It is therefore desirable to modify the system in some way to provide for quiescent states.

One way to accomplish this is to insert a third null state in the bang-bang actuator and to brake the system when the null zone is entered. Implementing a third state requires a significantly different actuation scheme and entails the addition of another clutch (for the brake) to the system. Furthermore, certain performance measures may be adversely affected, since the null state is a destabilizing influence.[3] The problem to be studied in this thesis is the design of a three-state clutch servomechanism to meet a prescribed set of specifications.

1b. Description of the System and Specifications

The servo actuator must position the control surface mechanically in proportion to the input signal. To accomplish this the method

*A bang-bang control element is defined here to be an actuator whose output changes from one of two symmetric states to the other when the actuating signal changes sign.

of control used by Cheney and Firodia will be employed, since their results seem to indicate its feasibility and applicability to the present problem. For our purposes the control surface need be positioned in one dimension only, and all positioning will be rotational. A schematic showing a generalized preliminary version of the control strategy is shown in Fig. 1b.1.* This schematic represents a slight departure from Firodia's suggestions in that the brake is on the output shaft rather than the clutch shaft; but it was felt that since the object is to trap the load in a quiescent state, braking the output shaft would be more effective.

The basic method of control operates as follows. After a sensor converts the angular position of the output shaft to an electrical signal, it is compared to the command signal, and the resultant error is fed to a three-state device through a compensation network. For purposes of generality, tachometric (velocity) feedback has been inserted, although it is hoped that in the interests of economy and simplicity this may be avoided. Velocity feedback will act as added damping in the overall system, since it will effect reverse switching (i.e., negative actuating signal for positive command) before the system actually arrives at the command position. The three-state device (which is left unspecified for the moment) is an electrical device whose output can assume one of three states. If the output is the plus state (indicating large positive error) the plus relay is energized, and similarly if the output is the minus state (large negative error) the minus relay is energized. Finally, if the error is small enough to fall within the null zone around zero, neither relay is energized and the brake is activated.

The driving discs are driven by the primary power source within the vehicle and rotate at a constant velocity W_c in opposite directions. The driven disc, whose shaft is concentric to the driving discs, may be engaged to the forward driving disc by the activation of the plus relay and may be engaged to the reverse driving disc by the activation of the minus relay. (Electromagnetic means are used to develop the engagement forces.) If neither relay is energized, the driven disc is not

*As shown in this figure, we hereafter refer to the two clutches composing the driving mechanism as "the clutch".

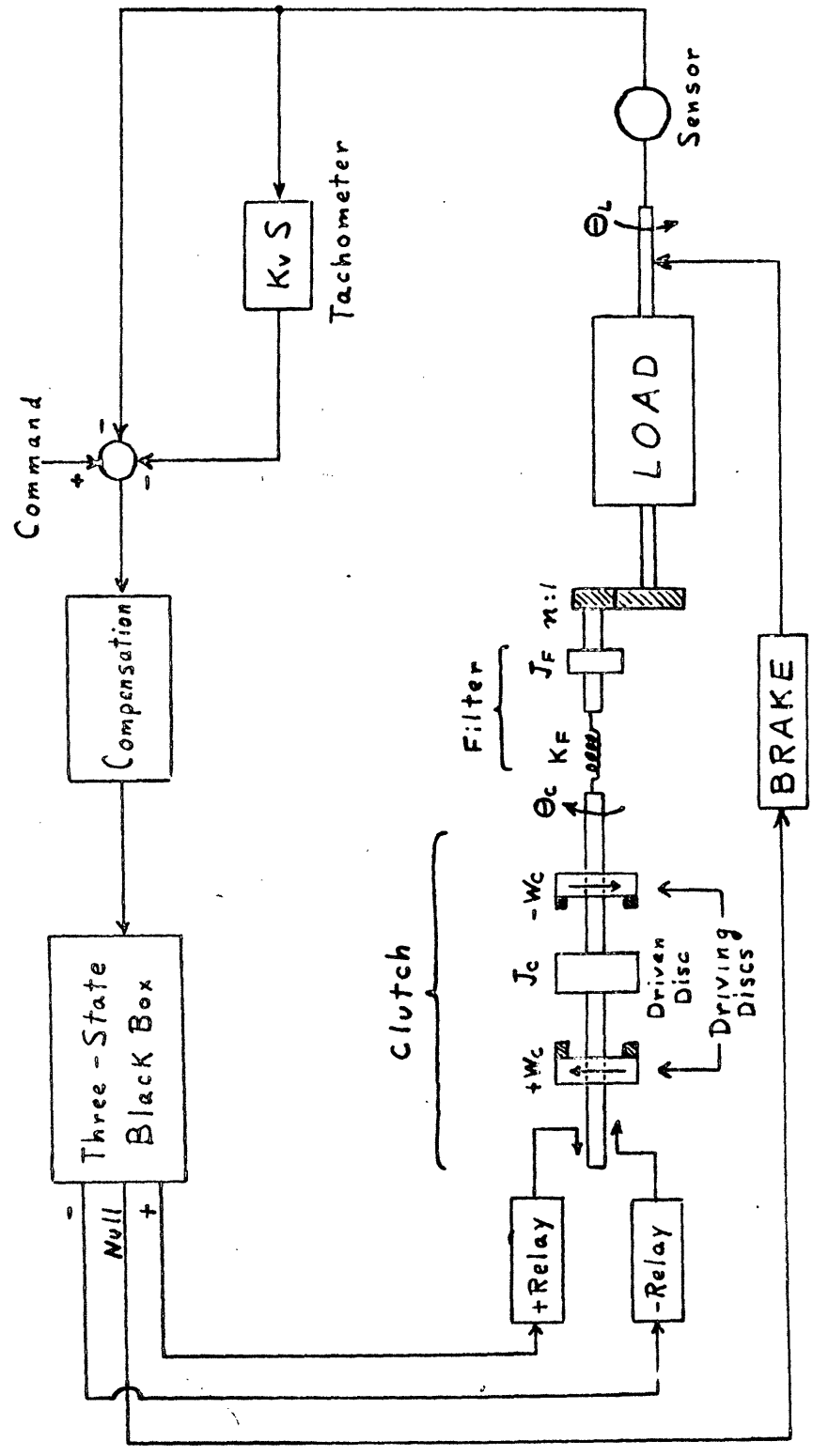

Fig. 1b.1 Schematic Diagram of the Control System

engaged and is allowed to drift free. The clutch shaft is connected to the load through a spring-mass filter and a gear train, both of which are employed to reduce torque requirements on the clutch. The system could be implemented without the spring ($K_F = \infty$), but this would make slippage a dominant factor in system performance and would require clutches with provisions for removal of large amounts of heat. The function of controlling the clutch (i. e., of providing driving currents) is to be performed by fast-acting electromagnetic relays or semiconductor switching circuits.[4]

Thus when the error indicates positive command, the driven disc should begin to rotate in the positive direction with velocity W_c, and the angle θ_c should increase linearly with time. When the error changes sign (due to velocity feedback and compensation), θ_c decreases linearly with time until switching again occurs or until the null state is reached. The step response of the system should therefore appear something like the curves of Fig. 1b. 2. It should be noted that the single-loop system shown in Fig. 1b. 1 is intended only as an exposition of the problem and will undergo some extensive changes later. The basic control strategy, however, will remain unchanged.

Although the load to be dealt with has not been specified yet, it would be well to introduce at this time the performance specifications[5] which the system must meet. They are as follows:

1. The small signal rise time should be less than or equal to 70 msec.

2. A small signal is defined to be a ±3. 5 degree input command.

3. Rise time is defined as the time the output takes in going from 10 percent to 90 percent of its final value when the input is a step function.

4. The peak magnification of the small-signal frequency response should be less than or equal to 1. 4.

5. This same frequency response shall be flat out to 7 cps or greater and shall have its -3 db point at 27 cps or greater.

6. Steady-state error should be no greater than 7 minutes of arc. (This is thought to be an excessively tight specification if an autopilot feedback loop is used around the servomechanism and the vehicle dynamics.)

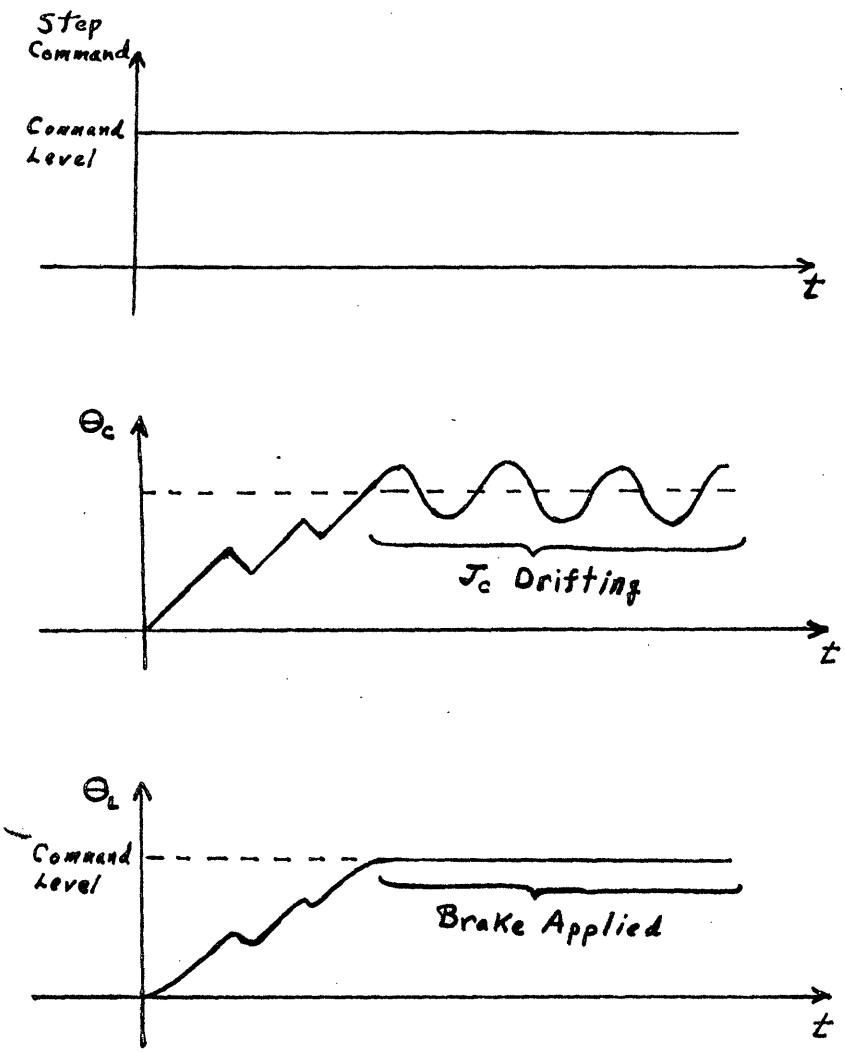

Fig. 1b.2 Expected Step Response of the System

1c. Research Objectives and Past Results

The objective of this work is the design and analog simulation of a three-state clutch servomechanism which satisfies the above specifications. Design may proceed freely in several areas, one of which is of course the selection of the three-state device in Fig. 1b.1. Variation of K_F, J_F, W_c, and K_v also offers design liberties, as does choice of compensation. Design work will be done chiefly through analog simulation, since a quantitative description of such a nonlinear system with several free parameters seems hopelessly complicated. Nevertheless, mathematical analysis is a further objective, and experimental work will be guided by as many analytical results as are obtainable. Experimental data will be used to verify analytical results.

It should be mentioned that the actual mechanical design of the clutch will not be attempted here. Rather a mathematical model of the clutch servo-system will be derived, and with this model overall system performance will be evaluated through analog simulation. Of course, the hope of eventually realizing the system must guide the design. One objective must be to keep switching to a minimum since heating in the clutches increases with switching rate. Another objective might be to keep K_F as small as possible in order to keep slippage in the clutch to a minimum. Such mechanical constraints must be considered with other primary objectives, and any results must be evaluated in light of these constraints.

Past results indicate the feasibility of the proposed system, although Firodia's optimum system does not meet all performance specifications. Firodia's system employs a control strategy very similar to that of Fig. 1b.1, with the exceptions that a two-state modulator replaces the three-state device and a switching delay of 1.0 msec. is assumed. The optimum system is able to meet all rise time specifications, but is at the limit of allowed peaking in the frequency response and is unable to meet bandwidth specifications. The two-state modulator used by Firodia is, however, not proposed for the system here, and thus the inherent limitations on bandwidth imposed by this control will be avoided.

The parameter values of Firodia's system seem to be physically reasonable and should not prohibit realization of the system. Although

no indication is given of the switching required in the system, it is again hoped that elimination of the two-state modulator will significantly reduce switching. The steady-state oscillations of Firodia's optimum system are of magnitude 7 minutes, and thus it appears that a null zone of comparable width is possible. It also appears from Firodia's data that meeting rise time specifications will not be difficult.

1d. Summary of Results

An optimum system is proposed in Chapter IV which meets all of the specifications. The final schematic of this system differs slightly from Fig. 1b.1 in that a two-loop form is employed. One signal position error plus output velocity compensation is used for switching the drive clutch, while another uncompensated signal is used for error indication and for braking. System parameters seem to be physically reasonable, and switching in the clutch is minimized so that switching delay does not significantly affect performance. As verified in Chapter V, delays of up to 1.5 milliseconds only cause reduction in bandwidth and do not appreciably affect other performance measures.

The results obtained with this three-state, two-loop system appear to be superior to those obtained by Firodia. Peaking is greatly reduced in the frequency response, bandwidth is increased from 15 cps to 27 cps, and rise time is decreased from 70 to 20 milliseconds. Compared with the two-state system switching is evidently decreased, and, above all, steady-state oscillations are eliminated. These results are summarized in Figs. 4c.3, 4c.4, 5a.4, and 5a.5. The final system schematic is given in Fig. 4c.1 and is repeated here in Fig. 1d.1.

The results of the analysis and simulation studies certainly suggest that a hardware realization of the system be implemented, but some qualifications must be made. Switching speed of the drive clutches is crucial, and switching delay probably should not exceed 1.5 msec. for good performance. Slippage in the clutches can also add an effective delay, and this must be taken into consideration. In a typical small signal step response 3 or 4 switches will occur in the space of 15 msec., and the clutch must be capable of producing such

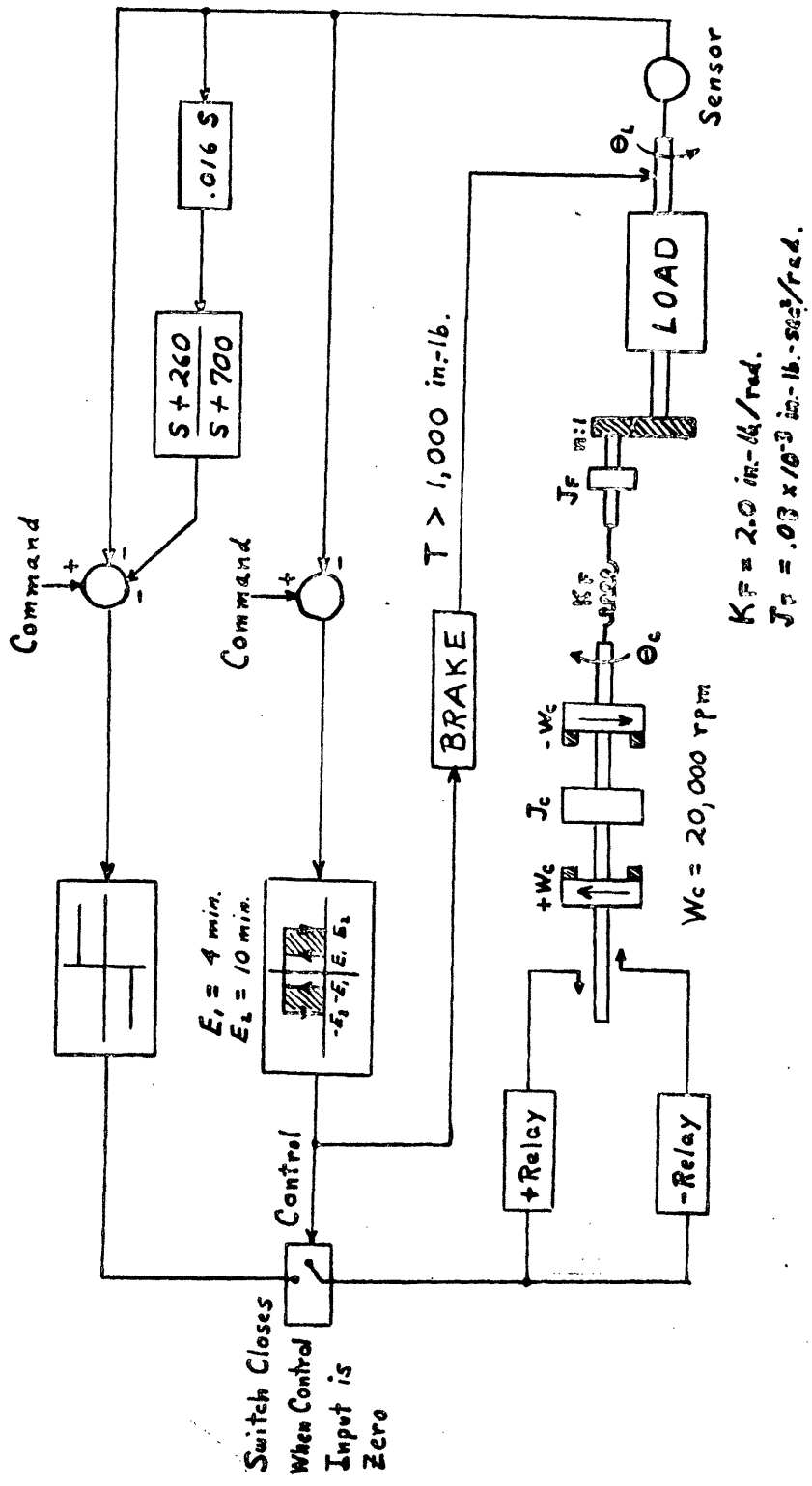

Fig. 1d.1 Schematic Diagram of the Optimum System

switching and if dissipating the accompanying small amount of heat. In addition, dissipation in the brake must be considered in relation to the size of brake required. In the simulation model, slippage did not appear to be significant but no quantitative results were obtained. In all studies the brake was assumed to have a maximum torque of 1000 in lb; obviously the number is reduced when the brake is placed on the other side of the gears.

The major strong points of the proposed system are its insensitivity to parameter changes and simplicity of the control components. The major weak points are the necessity of using three clutches rather than two and also the need for a tachometer in the feedback loop; however, the specifications for the system do not disallow such a tachometer. Designs which do not require a tachometer should be investigated further.

CHAPTER II

MODEL OF THE SYSTEM

In this chapter a simple mathematical model of the system is derived for use in analog computer simulation. In this preliminary model all delays and slippages in switching will be neglected. These effects will be investigated later in Chapter V.

2a Model of the Load

The load can be modeled as a second-order, lumped parameter system for the present study.[1] According to this model, the load may be thought of as a (rotational) spring-inertia-dash pot combination such as the one shown in Fig. 2a. 1. The equation of motion for the system is given by

$$J_L \ddot{\theta}_L + B_L \dot{\theta}_L + K_L \theta_L = T_L$$

where T_L is the external torque applied to the load and θ_L is the angular displacement of the control surface. The parameters J_L, B_L, and K_L, have the following values:

$$J_L = 0.05 \text{ in-lb-sec}^2/\text{radian}$$

$$B_L = 5.0 \text{ in-lb-sec}/\text{radian}$$

$$K_L = 2{,}000 \text{ in-lb}/\text{radian}$$

2b. Model of Clutch Shaft Velocity ($\dot{\theta}_c$)

As shown in Fig. 1b.1, the driven clutch disc may be engaged to either driving disc or may be left to drift. When the disc is engaged we shall assume (for the present) that the angular velocity of the clutch shaft immediately assumes the value $+W_c$ or $-W_c$ (as the case may be) independently of the previous shaft velocity. If the disc is allowed to drift we shall treat it as an ordinary inertia of magnitude J_c. Although the former assumption may seem rash at first, it must be recalled that the only clutch parameter which directly affects the load is the angular displacement of the shaft, θ_c. Thus, while a square wave approximation to $\dot{\theta}_c$ (see Fig. 2b.1) may be slightly unrealistic, regarding the integral of this curve as θ_c should involve

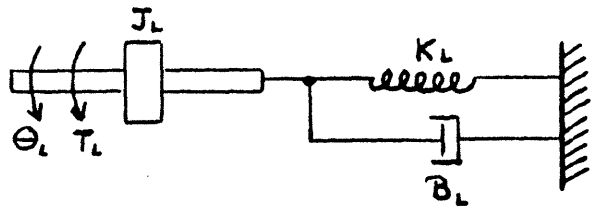

Fig. 2a.1 Schematic Diagram of the Load

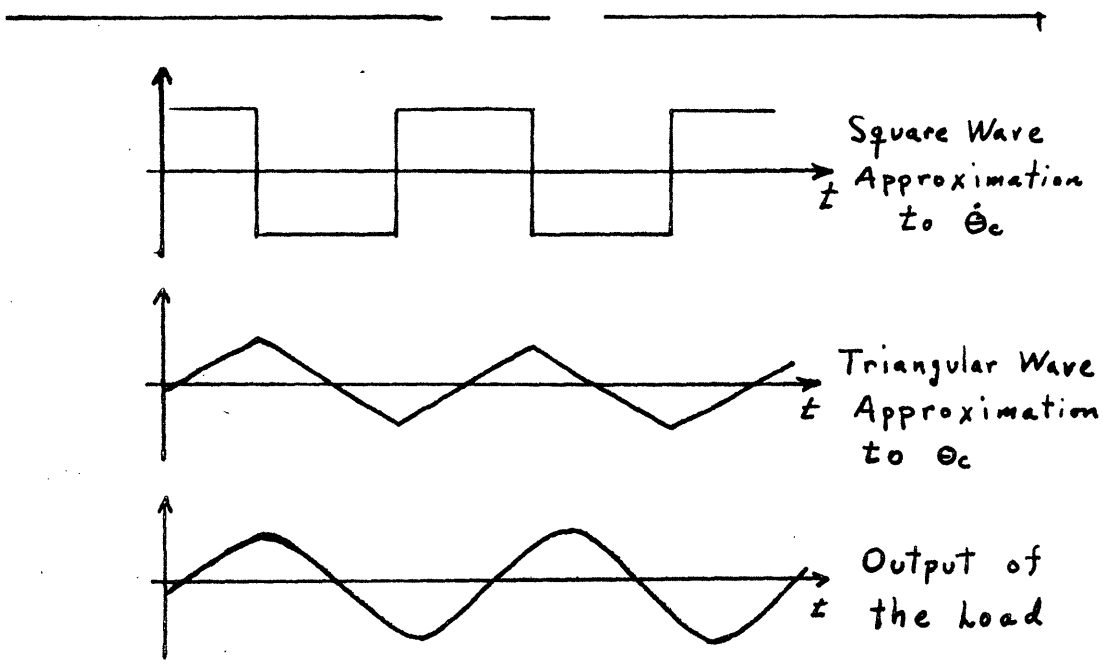

Fig. 2b.1 Approximations to θ_c and $\dot{\theta}_c$

only some sharpening of the peaks of a triangular wave and should not seriously affect load output (the load has low-pass characteristics). At any rate, these approximations will be employed for the present, and investigation of the effects of delay and slippage will be left to Chapter V.

2c. Derivation of System Equations

Let us isolate the clutch-load subsystem as shown in Fig. 2c.1. The following relations may be written from inspection of the figure:

$$K_F(\theta_c - n\theta_L) = J_F(n\ddot{\theta}_L) + T_1 \tag{2c.1}$$

$$T_L - T_D = J_L\ddot{\theta}_L + B_L\dot{\theta}_L + K_L\theta_L \tag{2c.2}$$

$$T_L = nT_1 \tag{2c.3}$$

Multiplying 2c.1 by n and using 2c.3, we obtain

$$nK_F\theta_c = n^2J_F\ddot{\theta}_L + n^2K_F\theta_L + T_L$$

Finally using T_L as given by Eq. 2c.2, we have

$$nK_F\theta_c = T_D + (n^2J_F + J_L)\ddot{\theta}_L + B_L\dot{\theta}_L + (n^2K_F + K_L)\theta_L \tag{2c.4}$$

This equation may be simplified by use of the following definitions:

$$\begin{aligned} J &= n^2J_F + J_L \\ B &= B_L \\ K &= n^2K_F + K_L \end{aligned} \tag{2c.5}$$

Thus Eq. 2c.4 becomes

$$nK_F\theta_c = T_D + J\ddot{\theta}_L + B\dot{\theta}_L + K\theta_L \tag{2c.6}$$

If the clutch is engaged to either driving disc, $\dot{\theta}_c$ is known to be $\pm W_c$ (as explained in Section 2b) and furthermore $T_D = 0$, since the

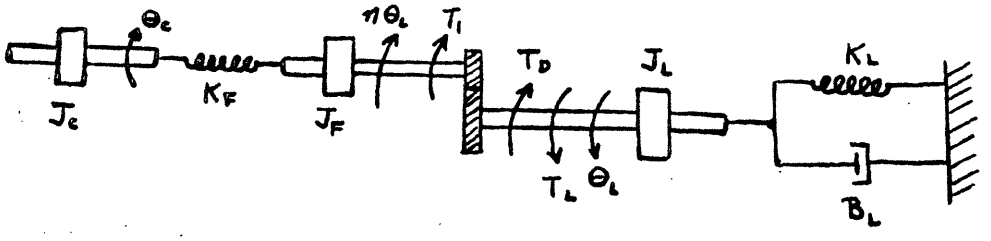

T_I = Total Torque Exerted on Inner Gear

T_L = Total Torque on the Load Shaft

T_D = Friction Torque Due to the Brake

Fig. 2c.1 Schematic Diagram of the Clutch-Load Subsystem

brake is not applied. Thus in this mode of operation (which shall hereafter be referred to as mode 1) Eq. 2c.4 is sufficient to specify the system output, as shown in the block diagram notation of Fig. 2c.2.

In mode 2, i.e., clutch disengaged from either driving disc, complications arise since $\dot{\theta}_c$ is no longer known. In this mode, however, no torque is exerted on J_c by the clutch, and we may write

$$K_F(\theta_c - n\theta_L) = -J_c\ddot{\theta}_c \qquad (2c.7)$$

When rearranged this becomes:

$$J_c\ddot{\theta}_c + K_F\theta_c = n K_F \theta_L \qquad (2c.8)$$

Using operator notation, we have

$$\theta_c = \frac{nK_F\theta_L}{J_c s^2 + K_F} = \frac{n\theta_L}{\tau^2 s^2 + 1} \qquad (2c.9)$$

Where we define τ by

$$\tau^2 = J_c/K_F \qquad (2c.10)$$

Combining Eq. 2c.9 with Eq. 2c.6, which is still valid in mode 2, we obtain

$$(Js^2 + Bs + K)\theta_L = \frac{n^2 K_F \theta_L}{\tau^2 s^2 + 1} - T_D \qquad (2c.11)$$

Since T_D, the brake torque, will be known in mode 2, Eq. 2c.11 is sufficient to specify the system output as shown in Fig. 2c.3. Note that by keeping the equation for $nK_F\theta_c$ in a separate block, we obtain a block diagram form which greatly simplifies the trading of initial conditions between the two modes. This will be extremely helpful in analog simulation.

The two Figs. 2c.2 and 2c.3 may be combined in a single block diagram provided that due care is taken to switch between the two modes of operation. The result is shown in Fig. 2c.4, where it is implied that initial conditions must be traded between the two sources of θ_c when a switch in mode occurs. Figure 2c.4 will form the

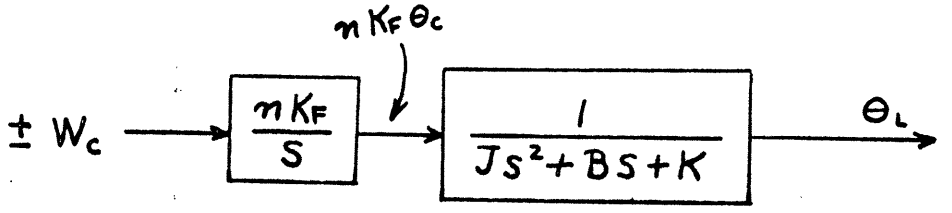

Fig. 2c.2 Subsystem Block Diagram for Mode 1 (Clutch Engaged)

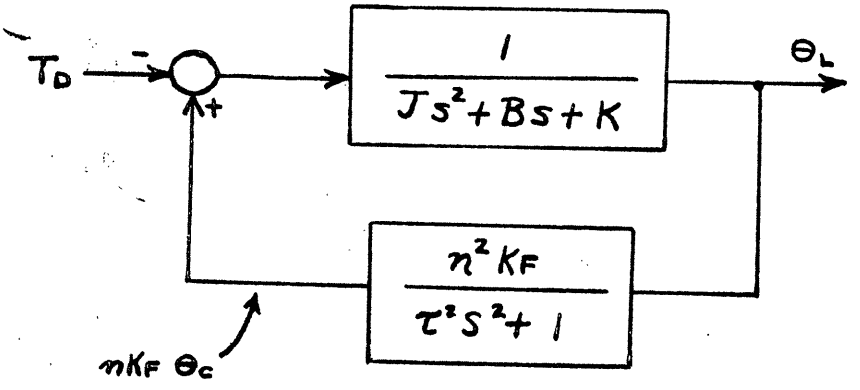

Fig. 2c.3 Subsystem Block Diagram for Mode 2 (Clutch Disengaged)

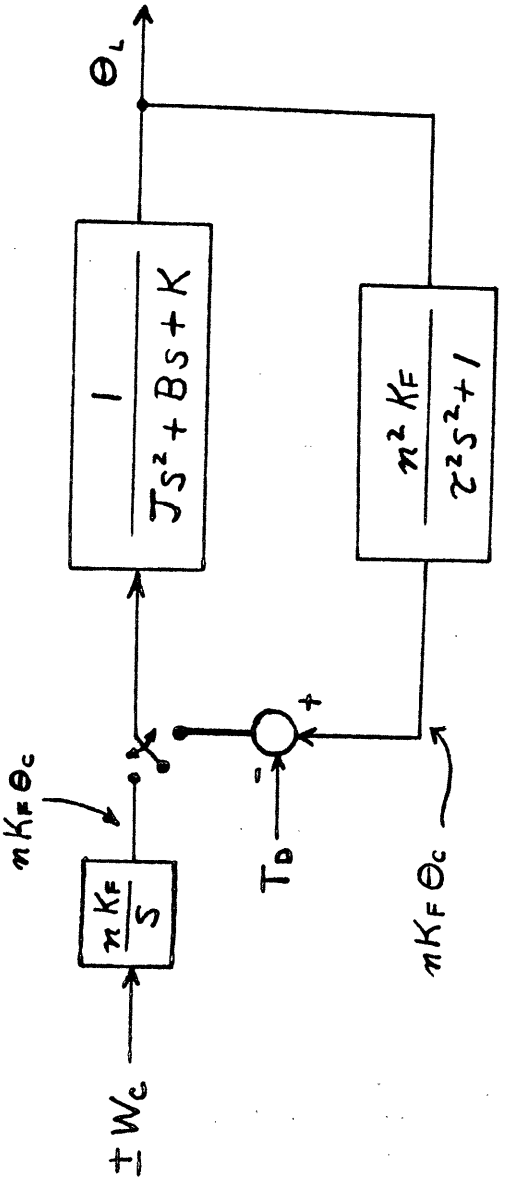

Switch Up = Mode 1 Switch Down = Mode 2

$J = n^2 J_F + J_L \quad B = B_L \quad K = n^2 K_F + K_L \quad \tau^2 = J_c / K_F$

Fig. 2c.4 Combined Block Diagram of the Clutch-Load Subsystem

basis for all analog simulation of the clutch-load subsystem and will remain unchanged through all future work. It is evident that the switching of modes and switching of sign of W_c must be produced by signals generated outside the subsystem, and indeed derivation of these signals is a major objective of the analog simulation.

2d. Model of a Friction Brake

Inspection of Fig. 2c.4 reveals that one additional model must be specified before analog simulation can proceed. The model for T_D, or the friction brake torque, must still be formulated. The model that will be used in all simulation is described by the equation

$$\begin{aligned} T_D &= T\frac{\omega}{|\omega|} \quad , \quad \omega \neq 0 \\ T_D &= 0 \quad , \quad \omega = 0 \end{aligned} \tag{2d.1}$$

where T is a positive torque constant which depends on the brake in question, and ω is the angular velocity of the shaft being braked (in this case $\dot{\theta}_L$). This equation accurately represents the kinetic behavior of a friction brake,[3] and is adequate here since we will not be concerned with static behavior. Assigning zero torque at zero velocity allows for quiescent states. Equation 2d.1 appears graphically in Fig. 2d.1, where for purposes of simulation it is indicated that the region of zero torque is not exactly of zero width. No effort will be made to set T at a specific value, but instead the minimum value necessary for good performance will be determined. With this model, then, simulation may proceed.

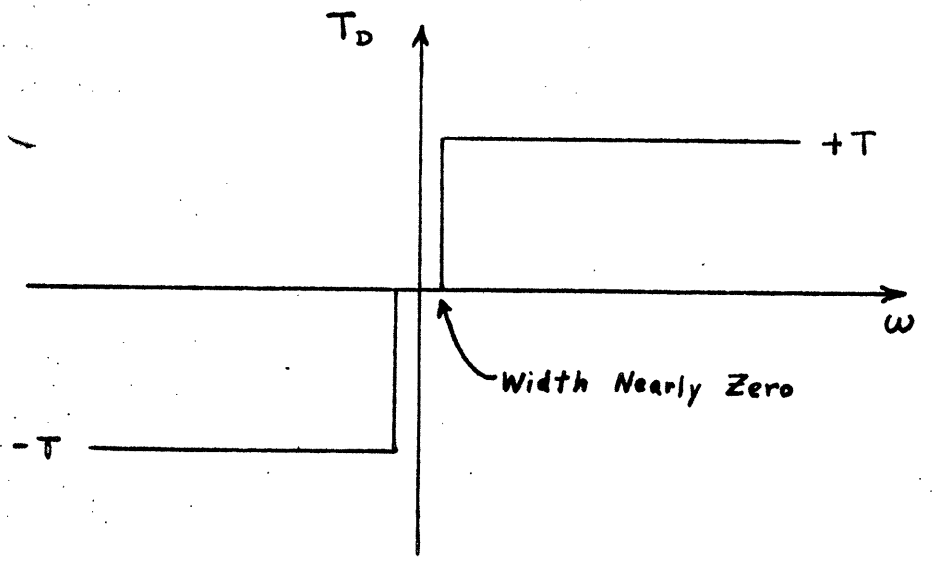

Fig. 2d.1 Model of a Friction Brake

CHAPTER III

ANALOG COMPUTER SIMULATION

In this chapter two approaches will be taken to the design of the three-state system, and the results of computer simulation will be presented. Free parameters initially will be given values which prove experimentally to be "good values" so that the better of the two systems may be chosen for optimization and further work. This better system will be analyzed in detail in Chapter IV.

3a. Analog Computer Symbols and Conventions

Before proceeding to specific systems, it seems advisable to introduce the analog computer symbols to be used in this paper. Figure 3a.1 lists the elements to be used and defines most of the conventions associated with them. Amplifiers and integrators are assumed to cause sign inversion, and for simplicity it will be assumed that both have an unlimited number of inputs. The gain of an amplifier or an integrator will be written in the center of its symbol, but any given input may assume a different gain if it is so indicated on the input lead, as shown in the figure. If an integrator is given no explicit initial condition, it is then assumed to be zero.

A comparator is a device which puts out a positive 10-volt signal if the algebraic sum of its inputs is negative, but gives zero volts output otherwise. A function generator of course may be used to approximate any curve, but in our case a function generator will always indicate an absolute value network as shown in Fig. 3a.1. C/A and A/C converters are simply devices for converting analog signals to logic levels (10 v. analog to logic one and 0 v. analog to logic zero). An electronic switch is a device whose normally open contact (indicated n o) is closed when the control is plus 6 v. and is open when the control is at 0 v. The normally closed contact (indicated by n c) of course is the inverse of the normally open contact.

With this list of elements at our disposal, we may proceed to form schematics of the simulation setups. It would seem advantageous, however, to begin by diagramming several of the basic building blocks

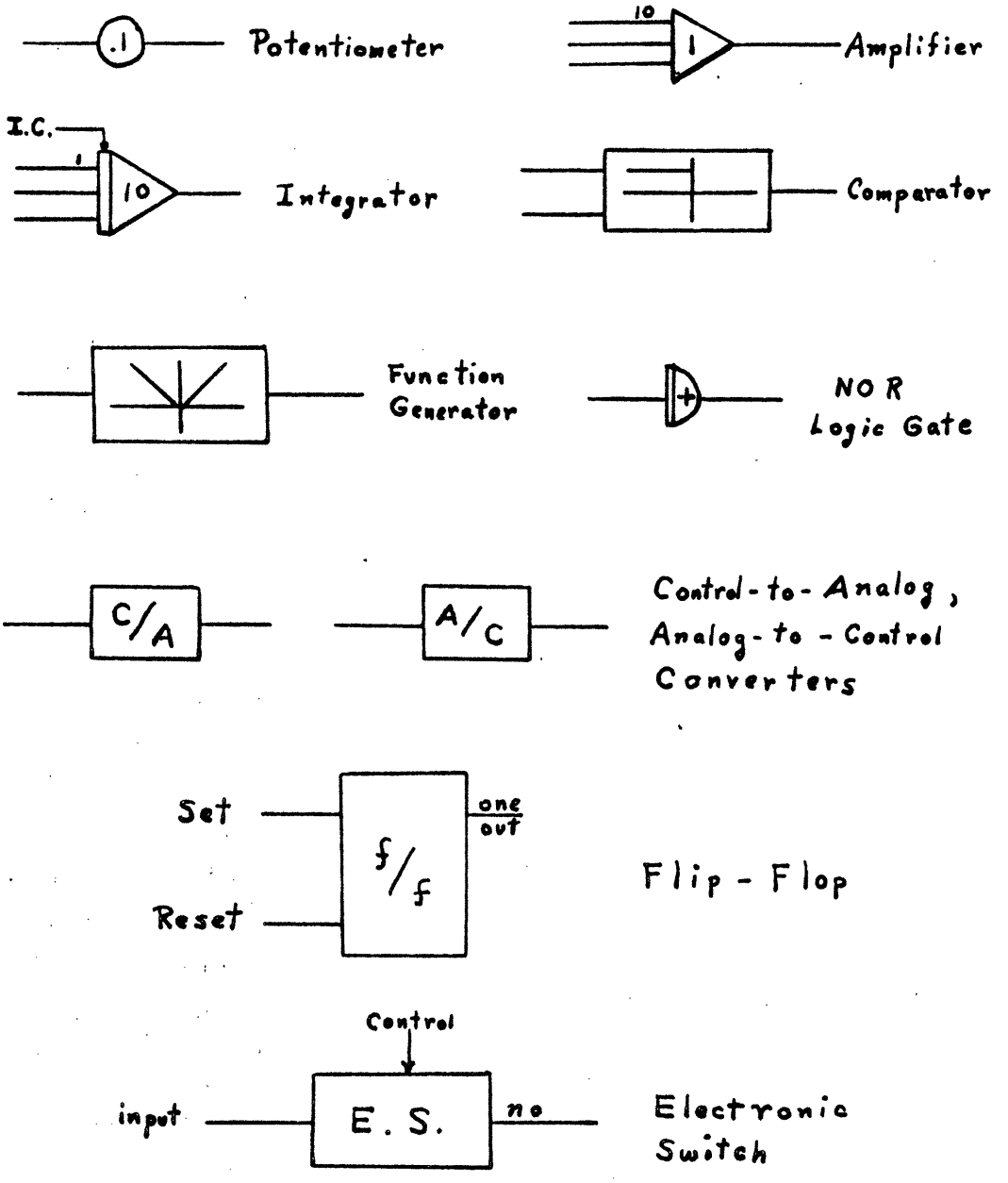

Fig. 3a.1 Analog Computer Symbols

to be used in future work. In this way complicated simulation diagrams may be built up from smaller blocks and still be kept reasonably small.

3b. Some Basic Simulation Building Blocks

A bang-bang device is easily simulated as shown in Fig. 3b.1. Hereafter any bang-bang device will be represented only by its block symbol (also in Fig. 3b.1). A phase lead compensation network may be simulated in the manner shown in Fig. 3b.2, where the corresponding block symbol is also shown. The integrator gain has been chosen as 1,000 since A will generally be in the range of 300-600. Note that $\alpha = 0$ is a possible special case of this method. The brake model of Fig. 2d.1 may be simulated as shown in Fig. 3b.3. In this circuit the comparator switching points are displaced slightly from zero, and the gain-of-ten amplifiers are used to insure that the region of zero torque is kept small. Figure 3b.4 shows the simulation of a three-state device with dead zone. The potentiometers, which ideally should be set at the same value, are used to fix the width of the dead zone. It should be mentioned that Figs. 3b.3 and 3b.4 are not identical because the range of adjustment of the comparators is not sufficient to permit a significantly large dead zone. Finally, Fig. 3b.4 may be combined with a function generator to produce an on-off device as shown in Fig. 3b.5. Note that the potentiometers still are used to set the overall width of the dead zone.

With these building blocks we are prepared to begin the simulation of specific systems.

3c. Simulation of a Single-Loop System

The obvious approach to designing the clutch is to insert a simple three-state device with dead zone in the black box of Fig. 1b.1. Such a system would appear schematically as shown in Fig. 3c.1, where the means of engaging the clutch is left implied. The block diagram corresponding to this system follows easily from reference to Fig. 2c.4 and is presented in Fig. 3c.2, where again it is implied that initial conditions must be traded when the switch changes position. From this block diagram one may proceed to the analog computer simulation

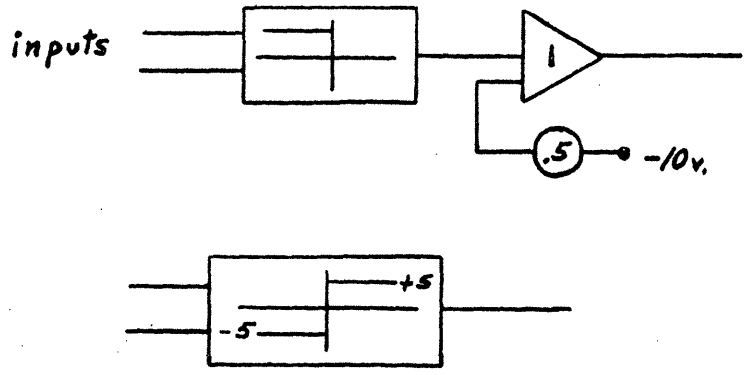

Fig. 3b.1 Analog Simulation and Block Symbol of a Bang-Bang Element

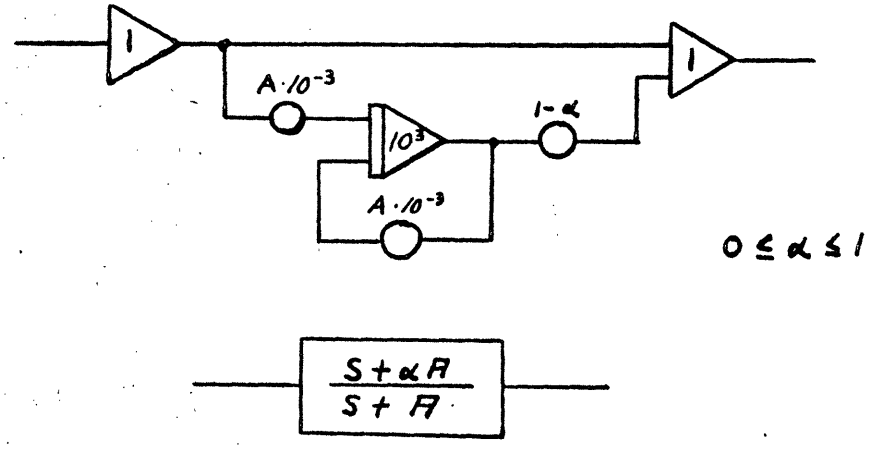

Fig. 3b.2 Analog Simulation and Block Symbol of a Phase Lead Network

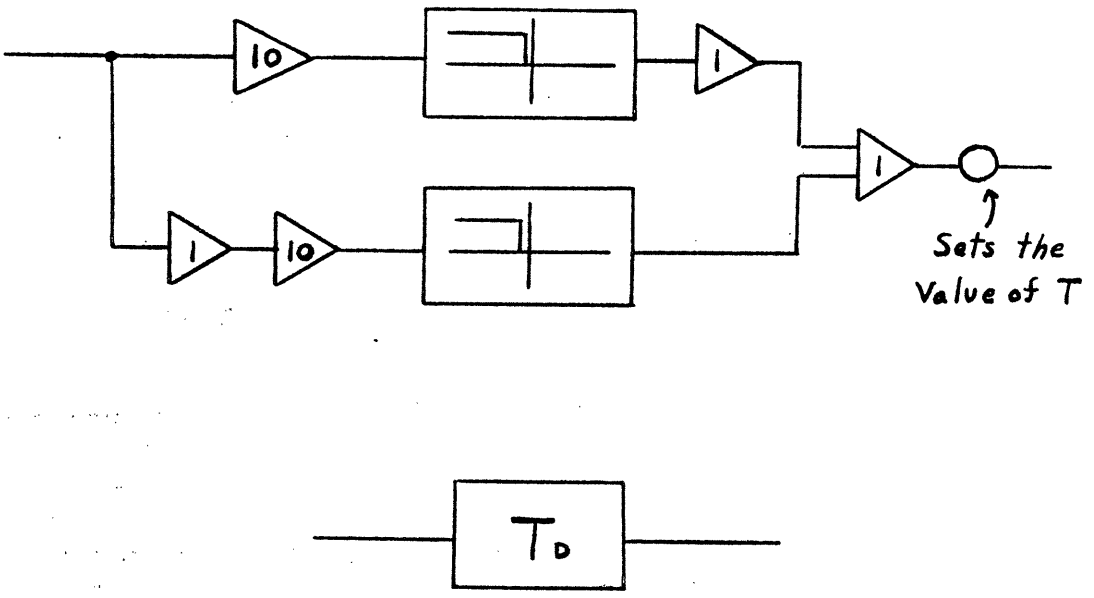

Fig. 3b.3 Analog Simulation and Block Symbol of the Brake Torque, T_D

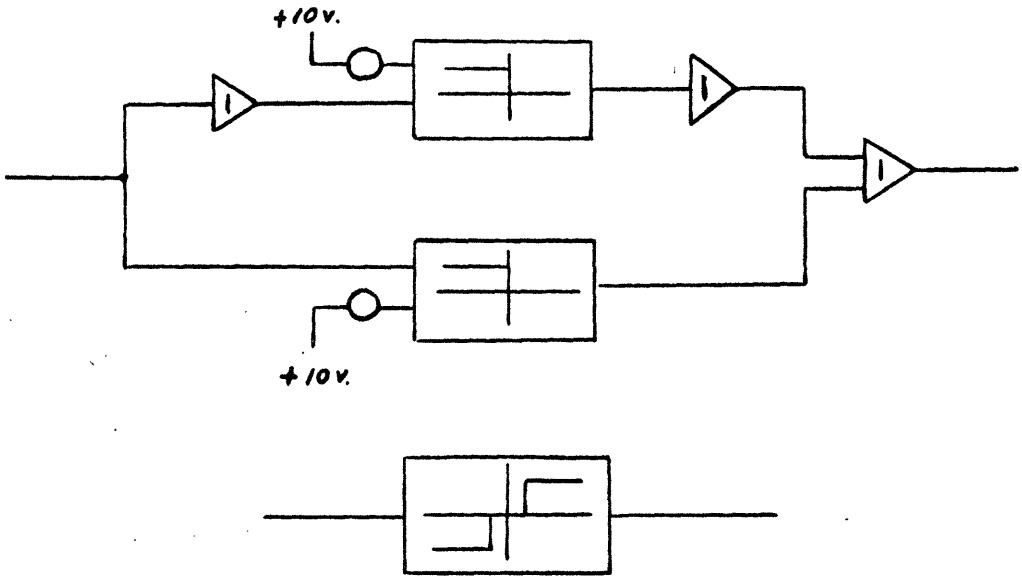

Fig. 3b.4 Analog Simulation and Block Symbol of a Three-State Device

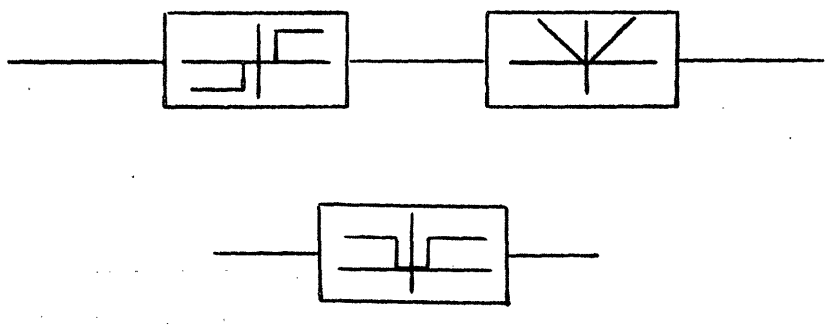

Fig. 3b.5 Analog Simulation and Block Symbol of an On-Off Device

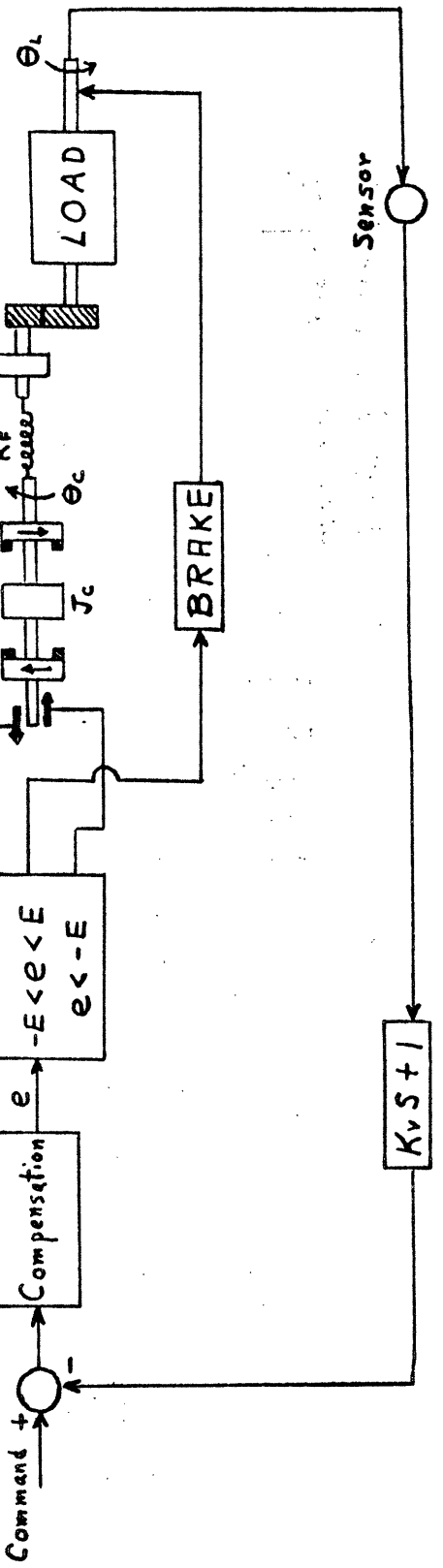

Fig. 3c.1 Schematic Diagram of the Single-Loop System

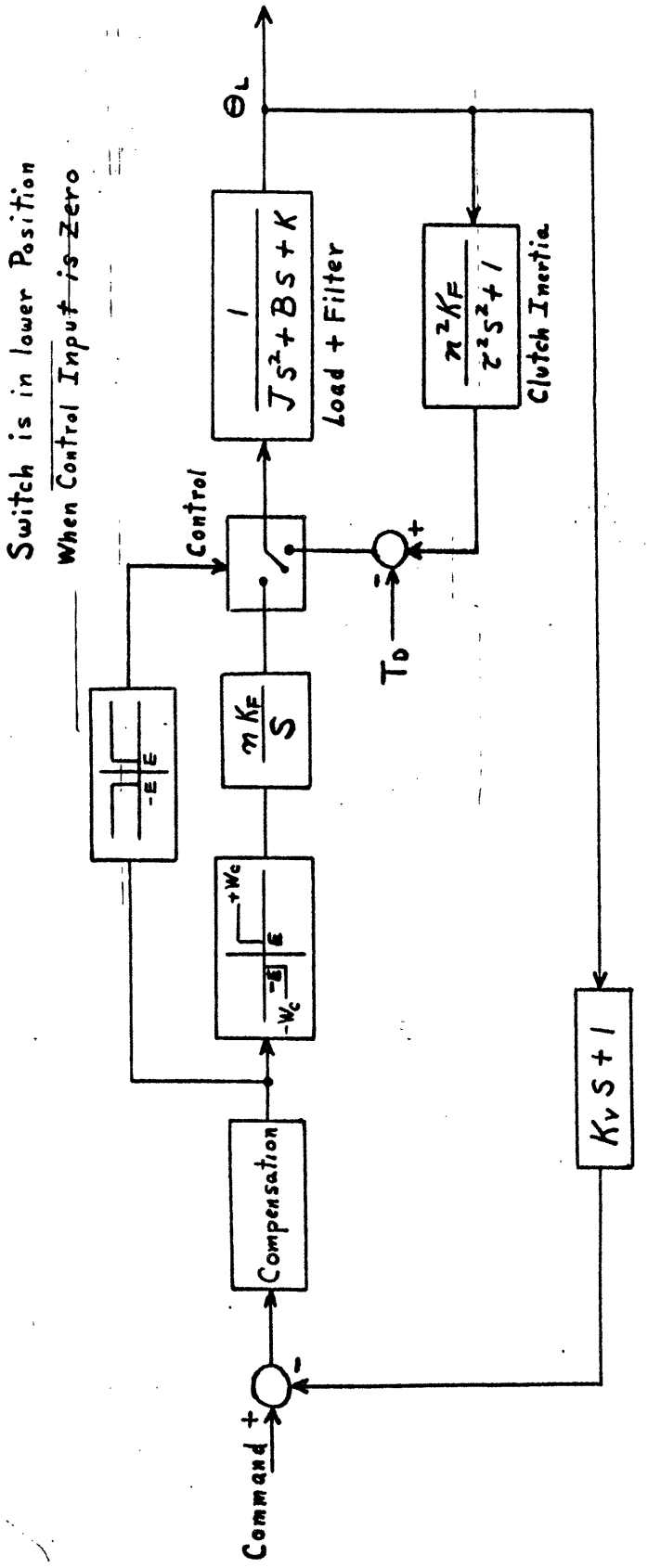

Fig. 3c.2 Block Diagram of the Single-Loop System

diagram given by Fig. 3c.3, although the transition may not be immediately obvious. The section including integrators I_3 and I_4 simulates the basic system equation appearing in the forward loop block of Fig. 3c.2 (i.e., the load plus filter). The central section including integrators I_1 and I_2 represents either the clutch inertia block of Fig. 3c.2 or the integrator block, depending on the state of the system. Switching of modes is controlled by the three-state device, but more elaboration is required on this point.

First, it must be explained that each integrator is governed by an EMC, or electronic mode control, which determines whether the integrator is in the integrate or initial condition mode. A positive 6 v. into the EMC places the integrator in the integrate mode and disconnects the initial condition input, while 0 v. into the EMC halts integration and switches in the initial condition input. Even though the tacit assumption has been made that all integrators are constantly integrating, it may be seen from the figure that this is not true for I_1, which changes modes as the system mode changes. When the system is in mode 1 (error outside the dead zone), I_1 is in the initial condition mode; but when the system changes to mode 2, I_1 changes to the integrate mode. Thus in mode 1 the output of the three-state device is fed directly to I_2 and is taken to be $\pm W_c$ (times a scale factor). (With an integrator gain of 1,000 the initial condition capacitor of I_1 is so small that the integrator behaves essentially like an amplifier with respect to its initial condition input.) In this mode, therefore, I_2 acts as the integrator block in Fig. 3c.2. In mode 2 of course I_1 and I_2 simulate the clutch inertia block of Fig. 3c.2. Thus the switching indicated in this figure is carried out as specified, and initial conditions are automatically correct.

The rest of Fig. 3c.3 is straightforward. T_D is applied to the load through the electronic switch only when the system is in mode 2. The A/C and C/A conversions, although seemingly superfluous, are necessary to supply power amplification for the particular applications. Lead compensation is used on the velocity feedback to minimize switching in the step response while maintaining significant damping at high frequencies. Thus, although the compensation represents a slight variation on the form of Fig. 3c.1, the schematic

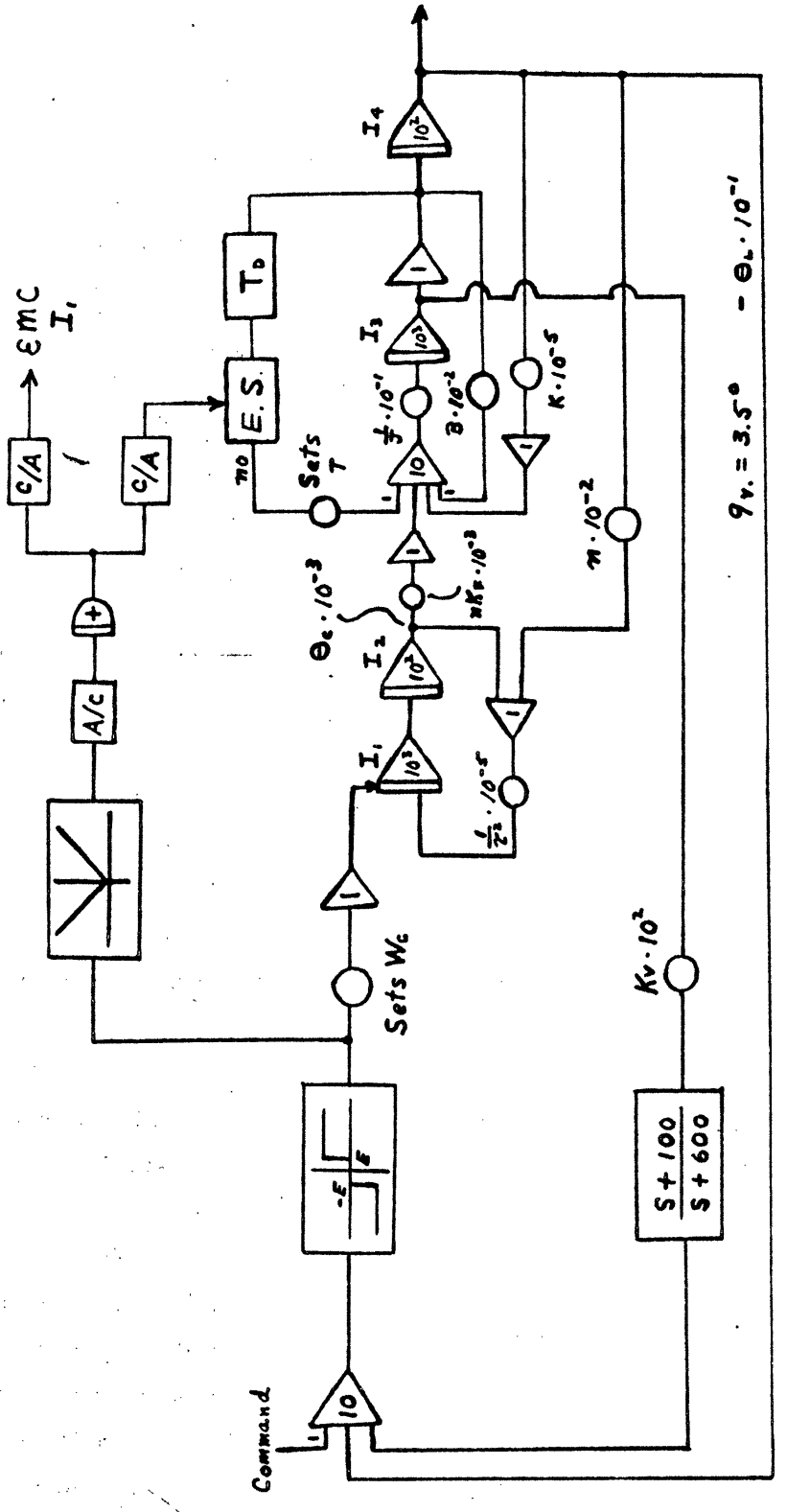

Fig. 3c.3 Simulation Diagram of the Single-Loop System

of this figure appears to be otherwise faithfully represented by the analog computer setup of Fig. 3c.3.

Figure 3c.4 shows some of the relevant waveforms observed in the simulation of this single-loop system with typical parameters. Although the small-signal step response is quite fast (20 msec. rise time) and well-damped, this good performance is achieved only at the expense of excessive switching. The small spikes visible in the switching waveform are actually the beginnings of the sinusoidal oscillations of J_c, caused by the system entering and leaving mode 2 repeatedly. Such switching implies rapid engaging and disengaging of the clutch at a rate (as can be seen) of about once per millisecond. This switching is not only a difficult requirement for any clutch suited to this system but is also extremely undesirable from the standpoint of efficiency. Decreasing the amount of velocity feedback of course reduces switching in the step response but a significant amount of velocity feedback was found to be necessary to maintain stability of the frequency response (i.e., to prevent uncontrolled oscillations) and to trap the system in the dead zone in the step response. Experimentally it was found that the velocity feedback coefficient could not be significantly reduced if a stable response was to be maintained. Furthermore, it was found that the system was very sensitive to variation in some parameters in that it tended to refuse to settle in the dead zone if, for example, K_v was too small.

The reason for this behavior becomes clear upon a closer examination of Fig. 3c.1. From the schematic it can be seen that slowing of the output shaft through reverse torque is impossible. That is, before the clutch can switch from one driving disc to another, presence in the dead zone will be indicated and braking will occur. Thus the step response will be a series of alternate driving and braking operations which will continue until the output reaches the command level. This type of behavior seems to be inherent in a single-loop system, since no parameter values could be found which would give satisfactory performance. Evidently the problem with this system is that it does not allow control of the load through reverse switching that is independent of error indication. Furthermore, it does not allow use of the brake solely when the output angle enters the dead zone. To

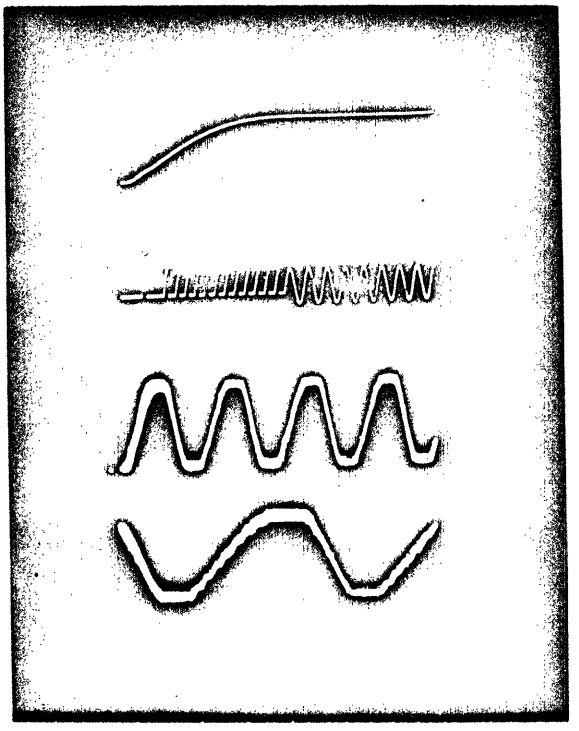

(a) Small signal step response. Duration of trace = 40 msec.

(b) Switching waveform ($-\dot{\theta}_c$) corresponding to trace (a). Duration of 40 msec.

(c) Small signal sinusoidal response at 2 cps.

(d) Small signal sinusoidal response at 7 cps.

Fig. 3c.4 Some Typical Waveforms for the System of Fig. 3c.1

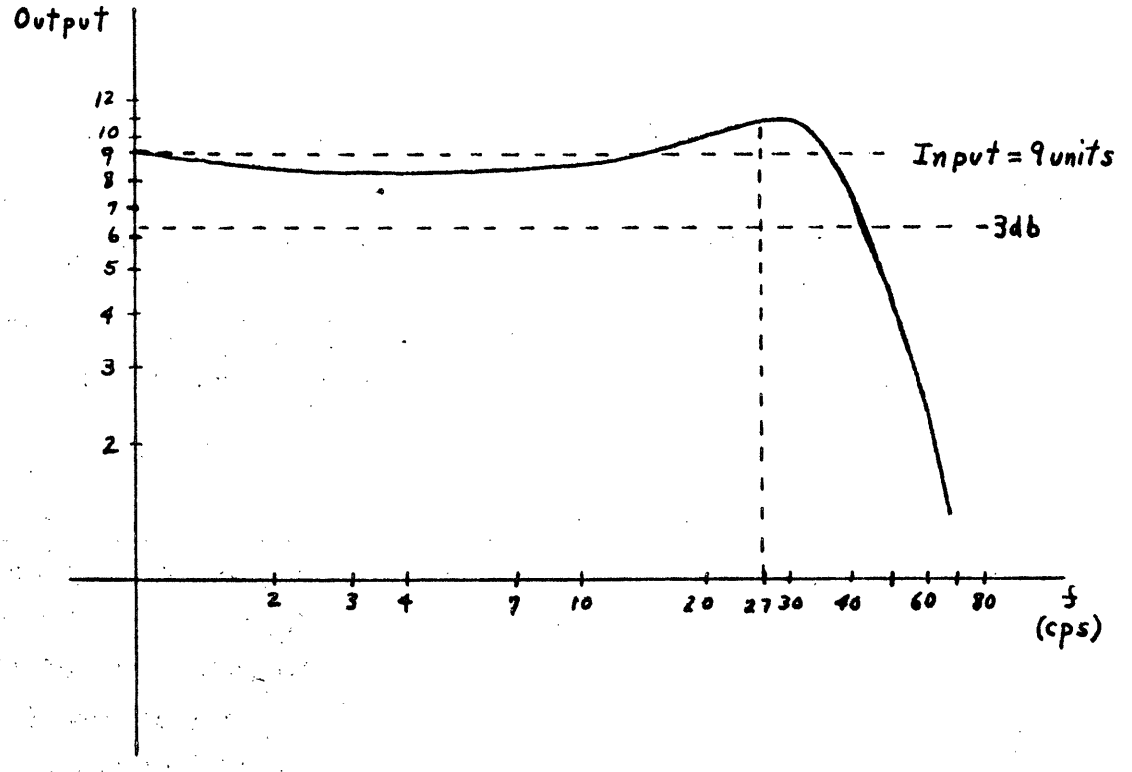

Fig. 3c.5 Typical Small-Signal Frequency Response for the System of Figure 3c.1

alleviate these defects, it would seem that a system employing two information signals, one for switching and one for error indication, is required. This will be the approach tried next.

Before trying another approach, one could of course try to improve the present system through better choice of parameters or through other means. As we shall see later, however, this single-loop system represents a very special case of the two-loop system that is simulated next, and this special case turns out to be far from optimum. Thus we may eliminate the single-loop system from further consideration.

3d. Simulation of a Two-Loop System

The system described in this section requires a slight variation on Fig. 1b.1, in that the single three-state device will be replaced by a pair of two-state devices with separate actuating signals. One of these devices, a bang-bang element, will control the switching of the clutch from one driving disc to another but will be incapable of leaving the clutch in a disengaged state. The second device, an on-off element with dead zone, will indicate error and will disengage the clutch and apply the brake only when error falls within the dead zone. Thus the error loop (referred to hereafter as the minor loop) determines whether or not the clutch should be driving or braking, and the switching loop (major loop) determines in which direction the clutch drives if it is engaged. The schematic of this two-loop system is shown in Fig. 3d.1 where it is indicated that the switch closes only when the error is outside the dead zone and that the brake is applied only during the inverse condition.

It may be seen that by choice of K_v larger than K_e and by appropriate choice of compensation, the system can be controlled through reverse switching without actually braking. In fact it was found experimentally that the best performance is achieved with no velocity feedback and no compensation in the minor loop - in other words, with nothing but straight error indication. (It should be mentioned, however, that this experimental conclusion does not consider constraints on the brake torque constant, T. In practice lead compensation may be required in the minor loop to induce some

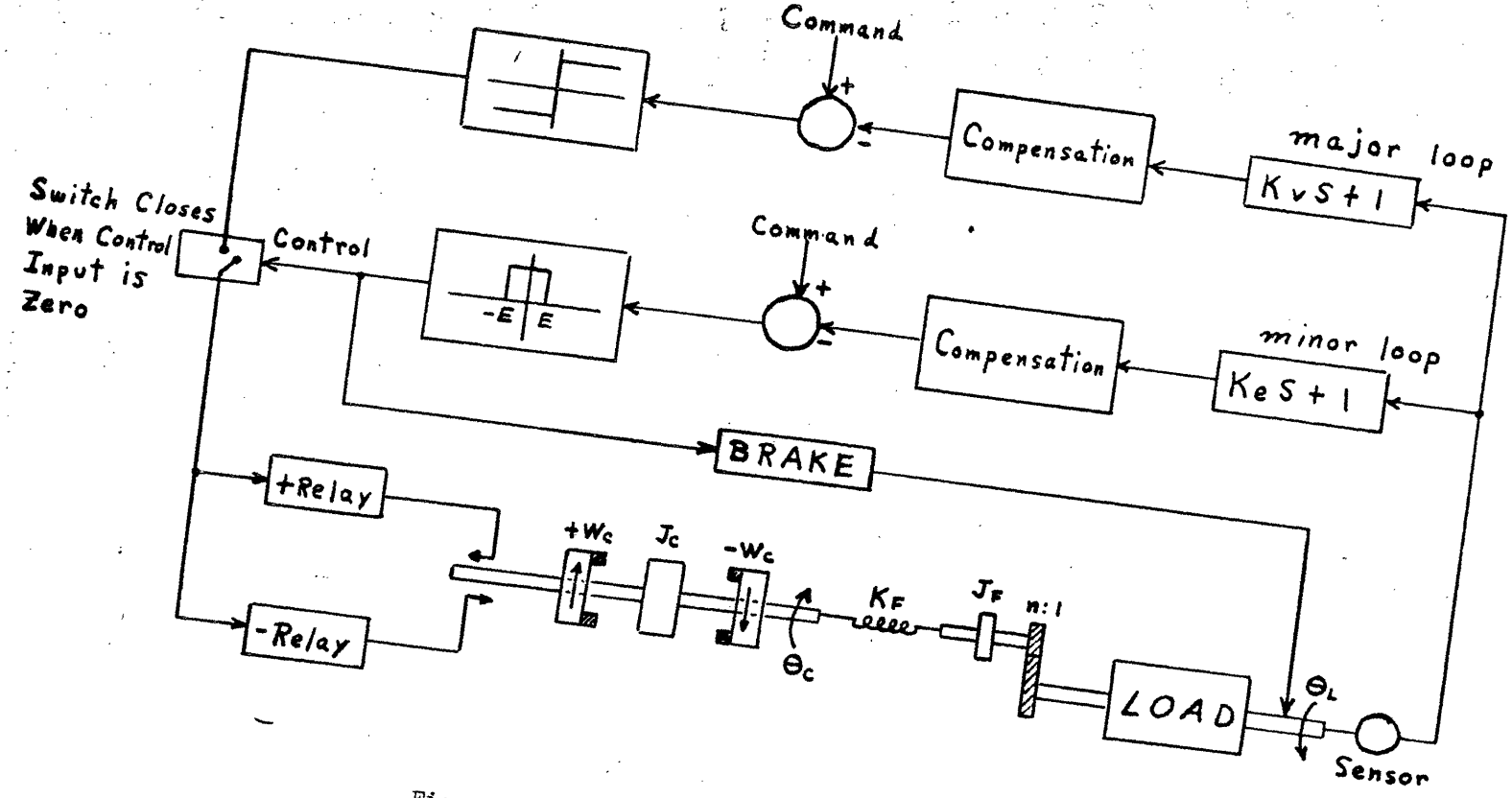

Fig. 3d.1 Schematic Diagram of the Two-Loop System

anticipatory braking if the brake is small.) Of course, K_v is significant in causing reverse switching.

With this in mind, then, the block diagram of the two-loop system may be presented as in Fig. 3d.2 where again trading of initial conditions is implied by the switching. The analog simulation diagram, which follows immediately from this block diagram, is presented in Fig 3d.3. The discussion pertaining to Fig. 3c.3 should be sufficient explanation for the new setup, since the two figures are quite similar. One may observe that again lead of the velocity feedback is the only compensation employed.

Some relevant waveforms observed in the simulation of the two-loop system are shown in Fig. 3d.4. Note that the step response is again quite fast (rise time 20 msec.) with no overshoot, but with this system no braking occurs until the output reaches the command level (braking occurs when the switching waveform becomes sinusoidal). Furthermore, switching is greatly reduced in the step response so that efficiency and heating are not compromised. The frequency response waveforms appear also to be smoother and more nearly sinusoidal, and peaking is reduced in the frequency response (see Fig.3d.5). In short, successfully meeting the specifications in a realistic manner seems much more likely with this two-loop system.

3e. Selection of the Better System

With the results obtained above there seems to be little difficulty in choosing between the two designs. Switching in the two-loop system is reduced to a realistic level with no loss in performance. In addition, this system shows much less sensitivity to parameter variations and therefore permits a greater flexibility in the design procedure. If there is any further doubt as to the superiority of the two-loop system, one further observation should resolve it. Reference to Figs. 3c.2 and 3d.2 shows that the single-loop system and two-loop system are separated by a small but significant difference; for if velocity feedback and compensation identical to that of the major loop were inserted in the minor loop, the block diagram of the two-loop system would reduce to Fig. 3c.2. As we have seen, however,

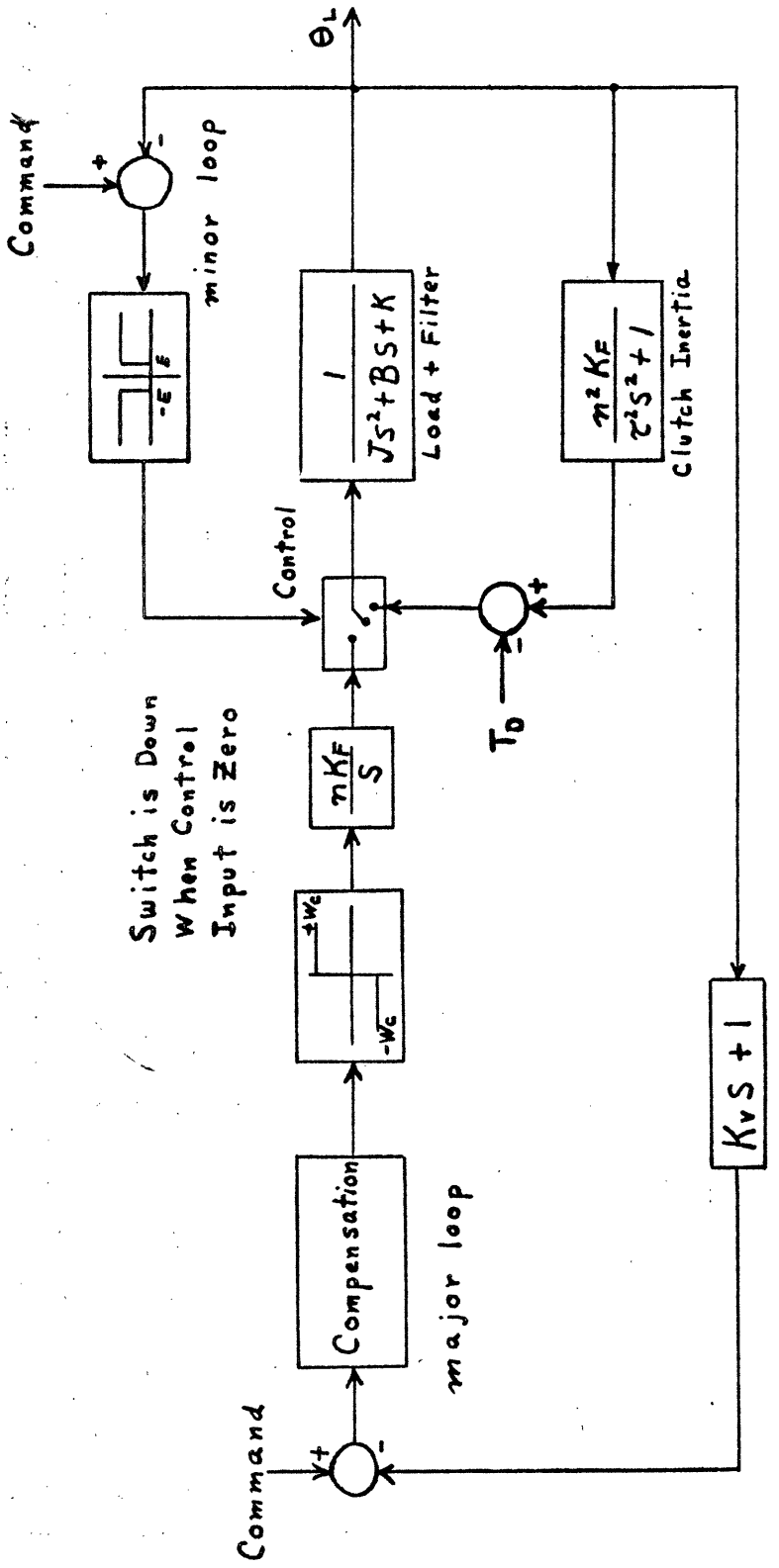

Fig. 3d.2 Block Diagram of the Two-Loop System

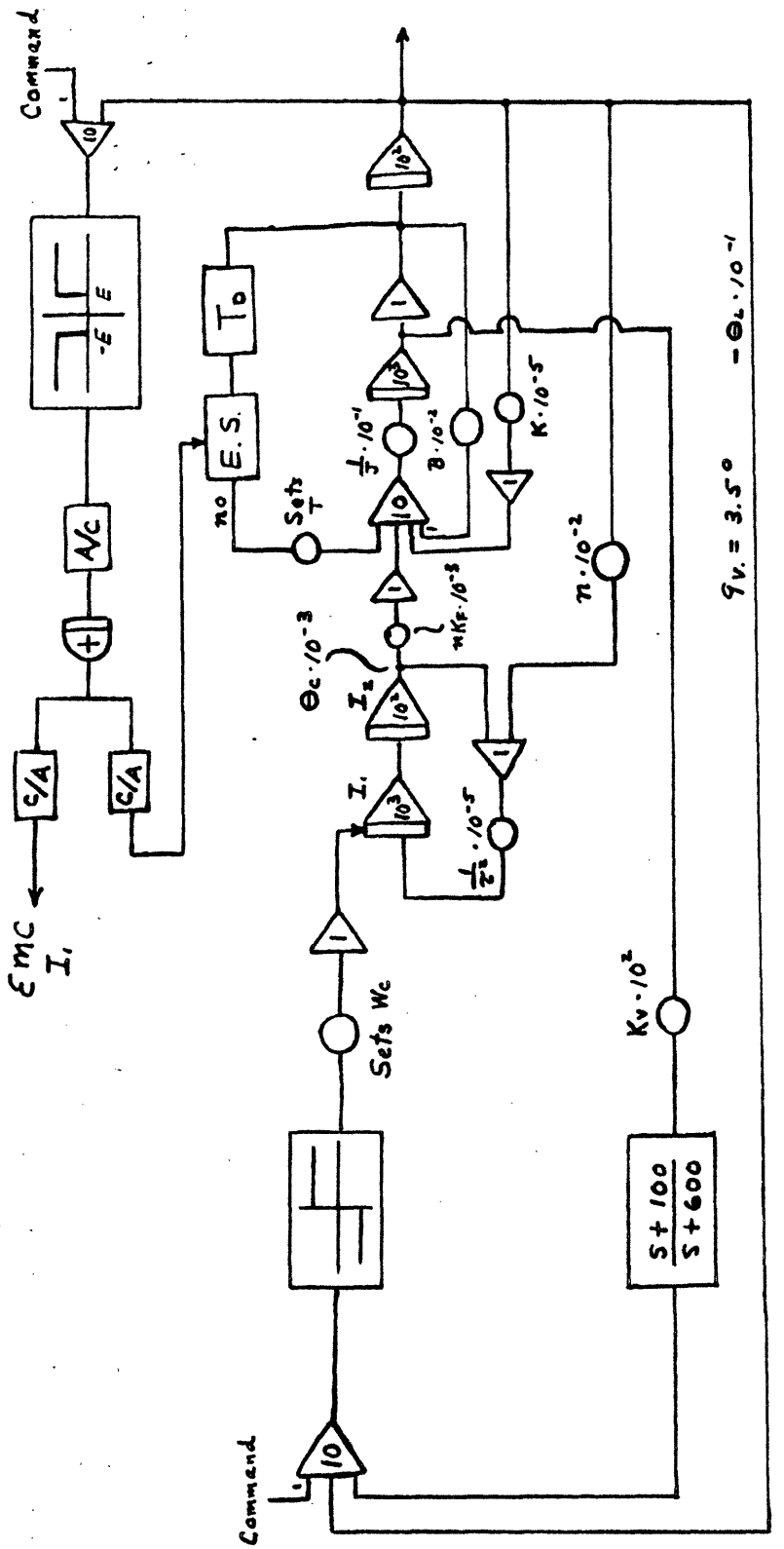

Fig. 3d.3 Simulation Diagram of the Two-Loop System

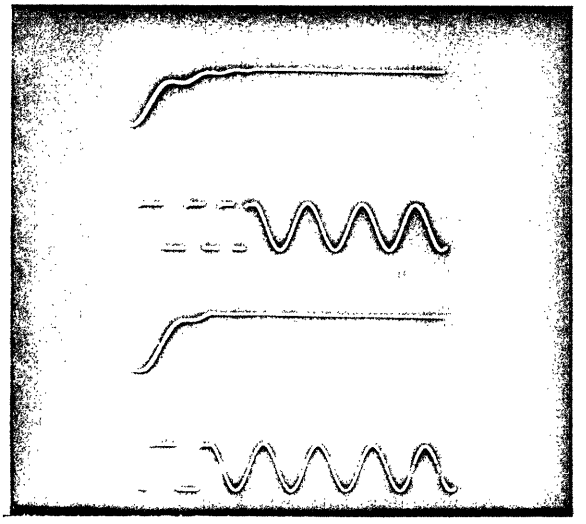

(a) Small signal step response. Duration of trace = 100 msec.

(b) Switching waveform ($-\theta_c$) corresponding to trace (a). Duration = 100 msec.

(c) Small signal setp response. Duration = 100 msec.

(d) Switching waveform for trace (c). Duration = 100 msec.

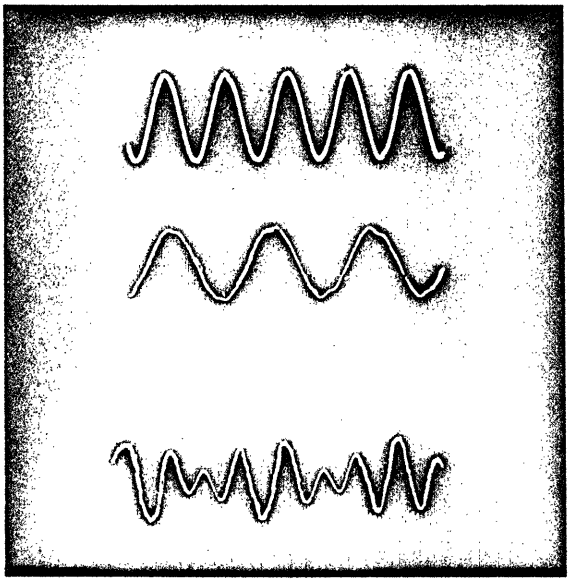

(e) Small signal sinusoidal response at 5 cps.

(f) Same at 15 cps.

(g) Same at 35 cps.

Fig. 3d.4 Some Typical Waveforms for the System of Fig. 3d.1

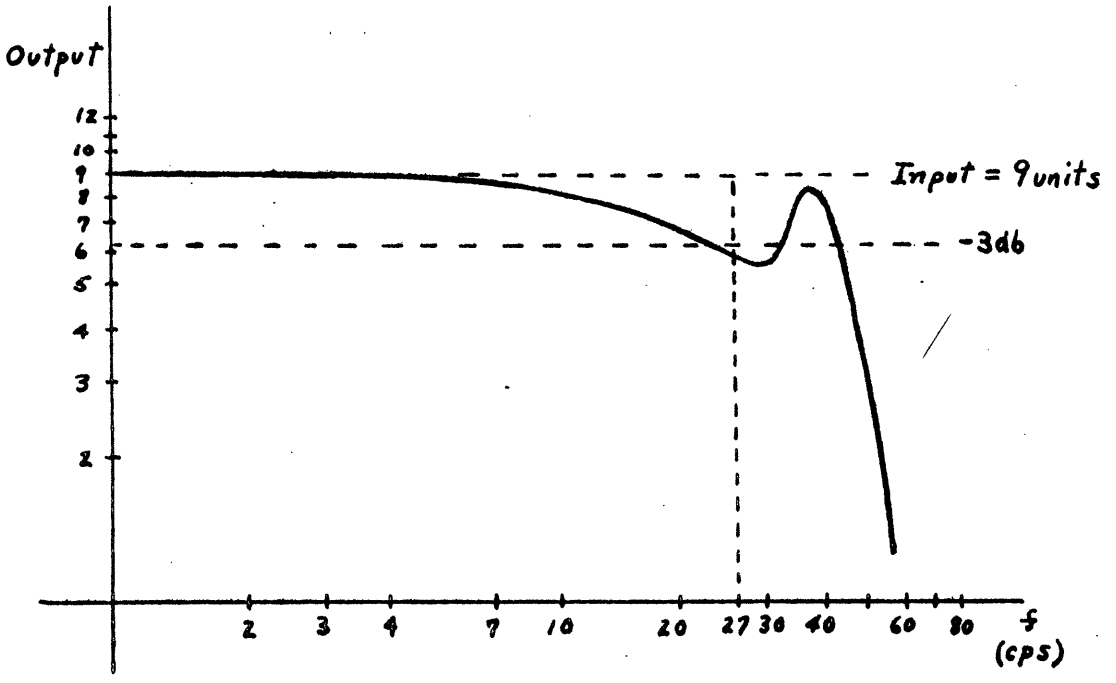

Fig. 3d.5 Typical Small-Signal Frequency Response for the System of Figure 3d.1

this special case is far from the optimum one. Consequently the single-loop system will be dropped from further consideration and all future work will center on the two-loop system of Figs. 3d.1, 3d.2, and 3d.3.

CHAPTER IV

THE SEARCH FOR THE OPTIMUM SYSTEM

In this chapter we shall attempt to optimize the two-loop system of Fig. 3d.1 through appropriate selection of available parameters. Optimization of course must be guided by the specifications given in Chapter I and must conform to principles of physical realizability. The method used here will consist of: (1) Analysis of the System, (2) Experimental Observation of Parameter Variation, and(3) Experimental Optimization. The most significant parameters available for design variation are the following:

Gear Ratio, n
Filter Spring Constant, K_F
Filter Inertia, J_F
Angular Velocity of Driving Discs, W_c
Velocity Feedback Coefficient, K_v
Width of Dead Band, E

In addition, of course, compensation networks may be inserted as seen fit.

4a. Analysis of the System

As was previously done, lead compensation will be chosen for the velocity feedback in the major loop in order to reduce high frequency peaking while maintaining a low level of transient switching. (Initially, lead compensation of the error signal was employed, but this form of compensation could not prevent high frequency peaking without inducing excessive transient switching.) For purposes of experimentation, we will find it convenient to split the lead compensation into a constant component and high frequency component as follows:

$$K_v \frac{s+\alpha A}{s+A} = K_{v1} + K_{v2} \frac{1}{s+A} \qquad (4a.1)$$

where $K_v = K_{v1} + K_{v2}$ and $\alpha = \frac{K_{v1}}{K_{v1} + K_{v2}}$

With this convention and with the velocity feedback of the minor loop set to zero (velocity feedback in the minor loop simply leads to unnecessary braking) the resulting system block diagram becomes that of Fig. 4a.1.

In this figure a new device is introduced which will be employed in all future simulation. A form of hysteresis has been inserted into the minor loop to help trap the system in the dead zone in the step response. With this device the system will not enter the dead zone until the error is less than some value E_1, but the system cannot leave the dead zone (once it has entered) until the error exceeds some value $E_2 > E_1$. The value of this innovation is that it forces the system to rest near zero error rather than on the edge of the dead zone, thus resulting in a more stable steady state. We will have more to say about the effects of this hysteresis later in the chapter.

It has been mentioned previously that since an analytic solution to this problem is hopelessly complicated, trial-and-error by analog simulation will be used as the design method. We should like, however, to guide the design by as many analytic tools as are at our disposal. First, looking at the load-filter subsystem of Fig. 4a.1 we see that this block is represented by a linear second order differential equation whose damping ratio, ζ and natural frequency, ω_n, are given by the conventional definitions as:

$$\zeta = \frac{\frac{1}{2}B}{\sqrt{KJ}} = \frac{\frac{1}{2}B_L}{\sqrt{(n^2K_L+K_2)(n^2J_L+J_2)}} \tag{4a.2}$$

$$\omega_n = \sqrt{\frac{K}{J}} = \sqrt{\frac{n^2K_F+K_L}{n^2J_F+J_L}} \tag{4a.3}$$

From Eq. 4a.2 we see that even if the values of n^2K_F and n^2J_F were negligible with respect to K_L and J_L respectively, the damping ratio ζ would only assume the value:

$$\zeta = \frac{1}{2}B_L(K_LJ_L)^{-1/2} = .25 \tag{4a.4}$$

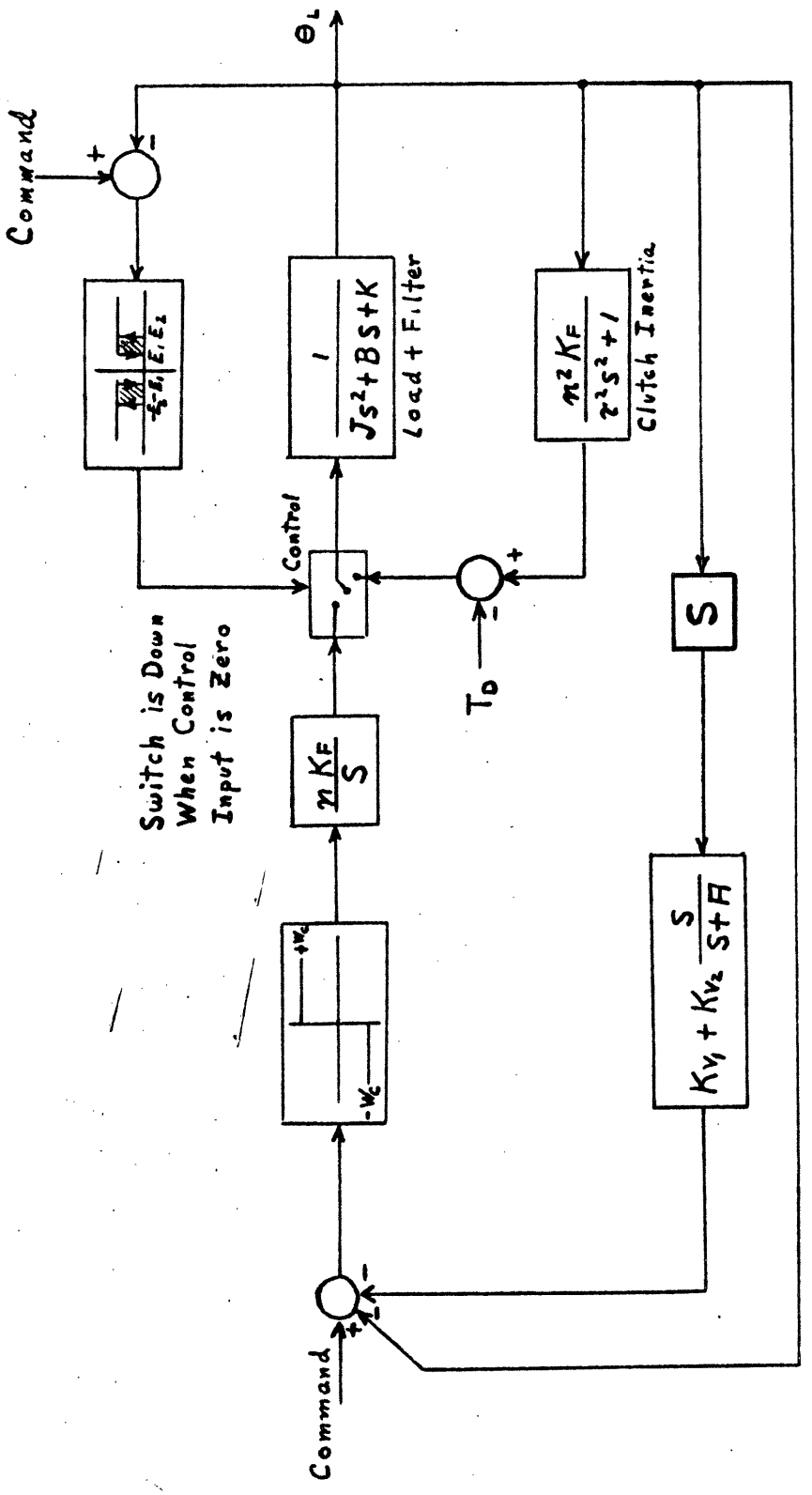

Fig. 4a.1 Block Diagram of the System to be Optimized

Since this is an essentially unattainable upper limit on the damping ratio, we must be resigned to an oscillatory response of the clutch-load subsystem. Equation 4a.3 shows that the value of the natural frequency of the subsystem is quite flexible; but both from the point of view of speed of response and from the specifications on the frequency response, we should like ω_n to be large. Thus J_F should be chosen as small as possible in order to increase both the natural frequency and the damping ratio. On the other hand, K_F must be chosen as a compromise between the damping ratio and natural frequency.

The value of the gear ratio n is generally chosen from torque considerations; however let us investigate the dependence of other system characteristics on n. We see from Eq. 4a.2 that ζ will decrease rapidly with n, and therefore from this point of view n should be kept as small as possible. The behavior of Eq. 4a.3 with respect to n is not immediately evident but can be easily determined by taking the derivative as follows:

$$\frac{d(\omega_n^2)}{dn} = \frac{2nK_F(n^2J_F+J_L) - 2nJ_F(n^2K_F+K_L)}{J^2}$$

$$= \frac{2n(K_FJ_L - J_FK_L)}{J^2} \qquad (4a.5)$$

We see from this expression that unless the condition holds that $K_FJ_L \geq J_FK_L$, ω_n will be a decreasing function of n. If this condition does hold then ω_n will monotonically increase with n and will have a minimum value (at n=0) of $\omega_n = \sqrt{K_L/J_L}$. Since a natural frequency of this value (200 rad./sec. or 32 cps) is already more than sufficient for bandwidth specification, we see that even if ω_n increases with n it would still be to our overall advantage to keep n small.

The gear ratio is also important in determining the steady state gain of the load-filter subsystem. From Eq. 2c.6 we have:

$$\left.\frac{\theta_L}{\theta_c}\right|_{s.s.} = \frac{nK_F}{n^2K_F+K_L} \qquad (4a.6)$$

By differentiation it may be verified that this expression is maximized for a given K_F by choosing

$$n^2 = \frac{K_L}{K_F} \qquad (4a.7)$$

Serious deterioration of gain results if n^2 is not close to this value, and thus if K_F is to be small, n must unfortunately be kept reasonably large. Let us compromise by choosing $n = 50$. This should be sufficiently large to satisfy torque requirements and will give good values of K_F from Eq. 4a.7.

With $n = 50$, the value of J probably cannot be made arbitrarily close to J_L since $n^2 J_F$ will be significantly large. Let us take $J = .25$ in.-lb.-sec.^{2}/rad. as a hopefully attainable value, with the corresponding value of J_F being $.08 \times 10^{-3}$ in.-lb.-sec.^{2}/rad. With these values of n and J, we may rewrite 4a.2 and 4a.3 as

$$\zeta = \frac{0.10}{\sqrt{K_F + .80}} \qquad \omega_n = 100\sqrt{K_F + .8} \text{ rad./sec.}$$

We see that the choice of K_F must represent a compromise since the value of ζ is quite small while the natural frequency is not as large as we would like it to be. Letting $K_F = 1.0$ in.-lb./rad. (which is an approximate solution to Eq. 4a.7) we obtain

$$\zeta = .075 \qquad \omega_n = 134 \text{ rad./sec.} = 21 \text{ cps}$$

This value of ζ is quite small, but apparently ζ must be of this order of magnitude since if the natural frequency were much smaller, we would have little chance of meeting the bandwidth specifications given in Chapter I. It would seem, however, that with ζ in this range the choice of K_F should be dictated more by the natural frequency than by the damping ratio. For example, a factor of 2 increase in K_F results in 6 cps. increase in the natural frequency but does not reduce the damping ratio sufficiently ($\zeta = .06$) to change the character of system response. This observation will be verified in Section 4c.

Turning to other parameters, we note that the values of E_1 and E_2 are set primarily by error specifications. E_2 must not be too large, however, or the frequency response will suffer. Since the steady-state error is specified to be less than seven minutes, we may reasonably set E_1 = 4 min. and E_2 = 10 min. These values will prove experimentally to yield an effective dead zone of less than seven minutes.

Some insight may be gained into the effects of remaining parameters through a phase plane analysis of Eq. 2c.6.

We will attempt to derive optimum step response switching curves in order to determine how these curves depend on K_v, W_c, and ω_n. In mode 1 we have

$$\ddot{\theta}_L + 2\zeta\omega_n\dot{\theta}_L + \omega_n^2\theta_L = \frac{nK_F}{J}\theta_c \qquad (4a.8)$$

To simplify the analysis we will assume that $\zeta = 0$. This approximation is justifiable since transient oscillations will decay with $e^{-\zeta\omega_n t}$, and for the values of ζ and ω_n determined above $\frac{1}{\zeta\omega_n} \tilde{=} 100$ msec. Switching will generally occur at intervals of less than 10 msec., and thus the exponential terms may be approximately neglected in the solutions of interest.

Assuming an initial positive switch, the clutch angle is given by

$$\theta_c = W_c t + \theta_i \qquad (4a.9)$$

where the parameter θ_i is introduced to account for the initial uncertainty in θ_c due to oscillations of the clutch in mode 2. With this form for θ_c the solution to Eq. 4a.8 (with ζ=0) may be written:

$$\theta_L(t) = a(W_c t + \theta_i) - \frac{aW_c}{\omega_n}\sin\omega_n t - a\theta_i \cos\omega_n t, \; t \geq 0 \qquad (4a.10)$$

with $$a = \frac{nK_F/J}{\omega_n^2} = \frac{nK_F}{n^2K_F + K_L} \qquad (4a.11)$$

In deriving 4a.10 we have assumed that all initial conditions are zero since the system is braked before the switch to mode 1 occurs. An

alternate form for Eq. 4a.10 is the following:

$$\theta_L(t) = a(W_c t + \theta_i) - \frac{A}{\omega_n} \sin(\omega_n t + \psi) \qquad (4a.12)$$

where $$A^2 = (aW_c)^2 + (a\theta_i\omega_n)^2 \qquad (4a.13)$$

and $$A \sin\psi = a\theta_i\omega_n \qquad A \cos\psi = aW_c$$

We also have $$\dot{\theta}_L(t) = aW_c - A\cos(\omega_n t + \psi) \qquad (4a.14)$$

Equations 4a.12 and 4a.14 may be displayed on the phase plane as shown in Fig. 4a.2.

From this figure it is evident that the optimum point at which to switch to the opposite driving disc may vary considerably with the value of A. Ideally we would like the switch to occur at such a point that the system arrives at the required angle, θ_R, with zero velocity. As demonstrated in Fig. 4a.3, however, a good linear switching curve for one value of A may be far from ideal for another. Furthermore, the slope of the optimum switching line may vary with θ_R even for a given value of A. Thus, it appears worthwhile to derive some form of an optimum switching curve so that the best straight line approximation may be used.

We now assume that a switch to the counterrotating disc $(-W_c)$ occurs at some time, τ. For $t \geq \tau$, θ_c is given by

$$\theta_c = W_c(\tau - t) + W_c\tau + \theta_i$$

Thus Eq. 4a.8 may be solved again, with initial conditions given by 4a.12 and 4a.14, to yield

$$\theta_L(t) = aW_c(2\tau - t) + a\theta_i - \frac{A}{\omega_n} \sin(\omega_n t + \psi) + \frac{2aW_c}{\omega_n} \sin\omega_n(t-\tau), t \geq \tau \qquad (4a.15)$$

If switching occurs at any point in Fig. 4a.2 for which $\dot{\theta}_L \geq 0$, it may be verified from Eq. 4a.15 that at some angle, $\theta(t_o) > 0$, the output will achieve zero velocity. By equating $\theta(t_o)$ to the command angle, θ_R, we determine the optimum switching point for the step input θ_R.

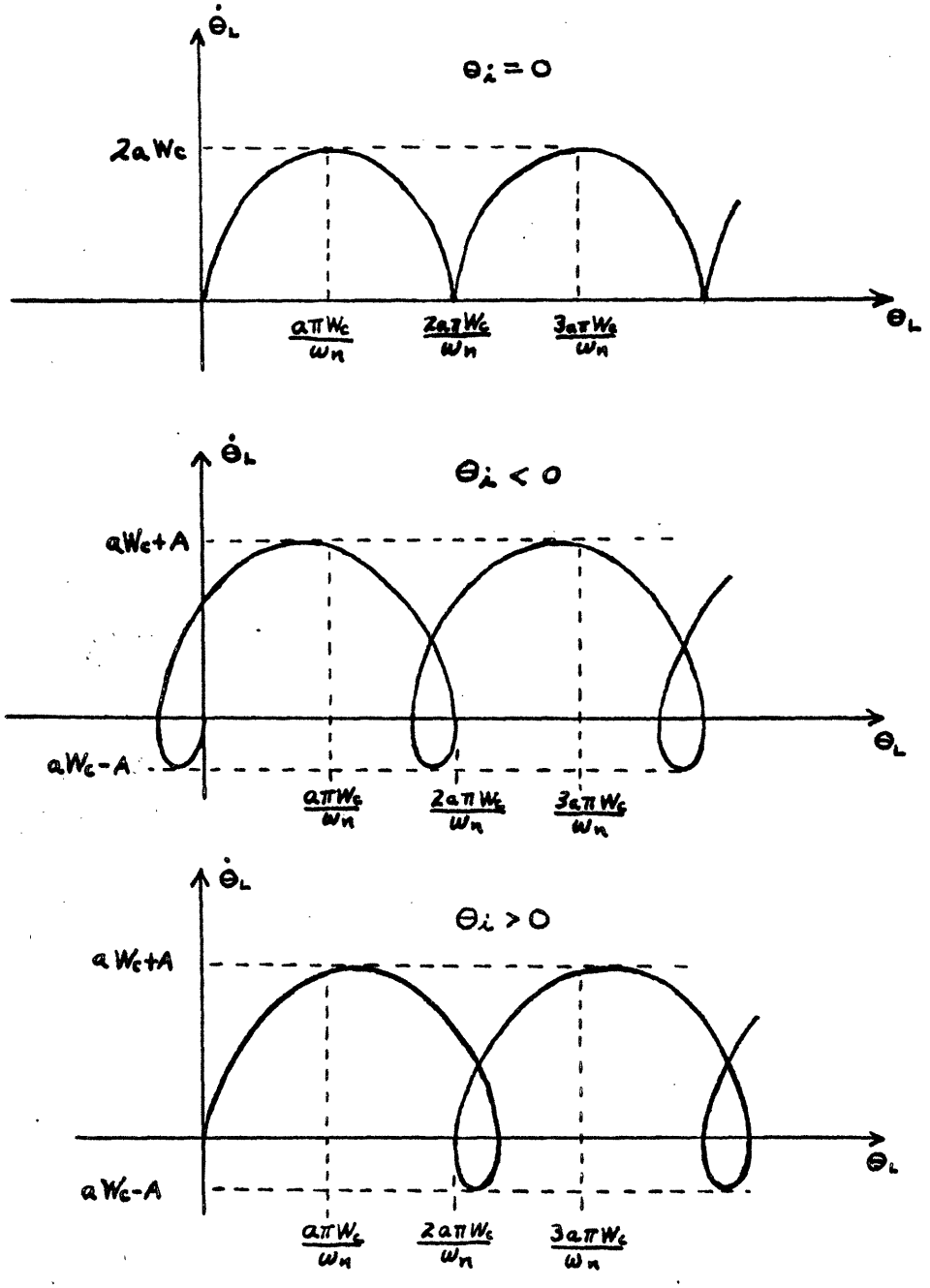

Fig. 4a.2 Phase Plane Plots of the System Equation

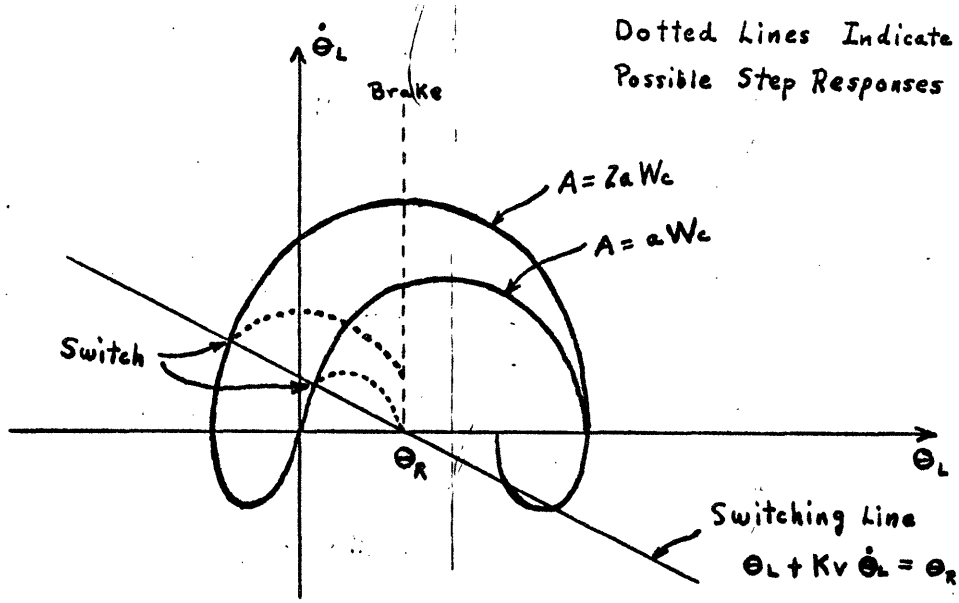

Fig. 4a.3 Step Responses for a Linear Switching Curve

By inserting several values of τ into Eq. 4a.15 and determining the corresponding $\theta(t_o)$, a set of optimum switching points may be generated. These points are most conveniently displayed on the phase plane in terms of the error signal defined by

$$E(t) = \theta_L(t) - \theta_R \qquad (4a.16)$$

With this notation the switching curves are a locus of the points

$$E(\tau) = \theta_L(\tau) - \theta(t_o)$$

$$\dot{E}(\tau) = \dot{\theta}_L(\tau)$$

In terms of the normalized error signal $\frac{aW_c}{\omega_n}E(t)$, the optimum switching curves are a function only of the amplitude, A. A set of these curves is presented in Fig. 4a.4 for various values of A with $\frac{\omega_n}{aW_c}\theta_R$ as a parameter. Parameter values are given only for $\theta_i > 0$ although for $A > aW_c$ a given point of the switching curve corresponds to two values of θ_R, one for positive θ_i and the other for θ_i negative. It should be noted that for $\theta_i > 0$ there is a minimum positive angle θ_R which can be reached at zero velocity after one switch.

Some conclusions may now be made from the curves of Fig. 4a.4. First it is apparent that unless $\theta_i=0$ we must be resigned to switching that is not optimum, and the system must arrive at some command angles with nonzero velocity. (The only way to circumvent this is to measure θ_c in addition to θ_L and $\dot{\theta}_L$.) If a linear approximation to the switching curves is to be used, then a conservative estimate is one which leaves the larger part of the curves above the line. One such line is shown in Fig. 4a.4, and for this line switching will be premature in most cases, causing the response to travel down the switching line to the vicinity of the origin. This at least places some constraint on the arrival velocity.

In Fig. 4a.4 it is apparent that the small signal portion of the $A=aW_c$ curve is closely represented by a straight line. It is also evident that as the ratio $\frac{aW_c}{\omega_n}$ increases, the linear portion of this curve represents a larger range of command angles. The maximum

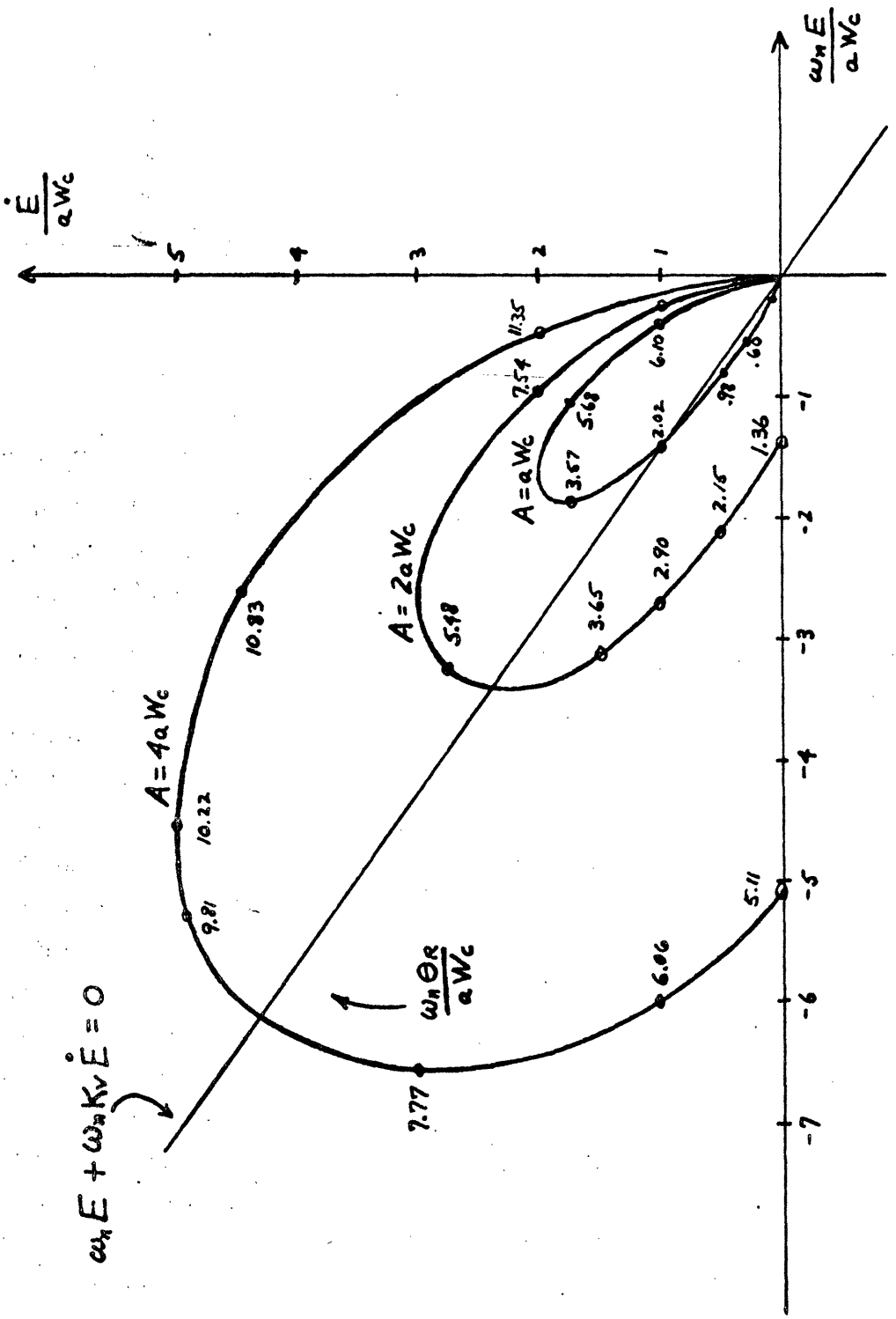

Fig. 4a.4 Optimum Switching Curves

input from zero is constrained to be 30 degrees, and if this angle is to be in the lower half of the curve, we see from Fig. 4a.4 that 30 degrees should approximately equal $3.57 \frac{aW_c}{\omega_n}$. For the parameter values arrived at earlier $a=1/90$ and $\omega_n=132$ rad./sec., and thus $W_c=1,740$ rad./sec. or approximately 16,000 rpm. We will initially set W_c equal to a more convenient value of 15,000 rpm and use 30,000 rpm as an upper limit. Such a limit is necessary since very large W_c may lead to excessive slippage, and, in addition, very high shaft speeds may be difficult to obtain.

Another important point of Fig. 4a.4 is that the slope of the switching line (i.e., the value of K_v) depends only on the system natural frequency, ω_n. The value of the product $\omega_n K_v$ is set by the normalized switching curves, and thus K_v varies inversely with ω_n for a given line. The line drawn in Fig. 4a.4 will be chosen for the initial switching line, since it is nearly optimum for small signal inputs if $\theta_i=0$, and since it appears to be a fairly conservative estimate in other cases. For this line and for the value of ω_n calculated previously, K_v is found to be .014 sec. With regard to the lead compensation of the velocity feedback, frequency response considerations will dictate parameters more fully later. For the present let us choose the high frequency breakpoint at 60 cps (about 400 rad./sec.) and the low frequency breakpoint at 30 cps. From Eq. 4a.1 this implies that $K_{v1}=K_{v2}=.007$ sec.

With these values for system parameters we may begin to test the effects of varying any given parameter. It of course would be a prodigious task to demonstrate simultaneous variation of two or more parameters, and for this reason we will vary one parameter at a time while the others remain fixed. The fixed-point values will be the following:

$K_F = 1.0$ in.-lb./rad.

$J_F = .08 \times 10^{-3}$ in.-lb.-sec.^{2}/rad.

$W_c = 15,000$ rpm

$K_{v1} = K_{v2} = .007$ sec.

$n = 50$

$E_1 = 4$ min. $\quad E_2 = 10$ min.

4b. Effects of Parameter Variations on Performance

With the fixed point, or reference, values given in Section 4a, we will attempt to determine through simulation how the system is affected by variation in individual parameters. Hopefully, these data will give us the knowledge necessary to select an optimum set of parameters. The system block diagram will not be presented here, since it is identical with Fig. 4a.1; however, the simulation diagram is given in Fig. 4b.1. (The method of simulating the hysteresis device has not been given previously and is presented in Fig. 4b.2.) In Fig. 4b.1 the breakpoint frequency of the compensation has been set at 400 rad./sec. (or 60 cps) since peaking generally will be found to occur in the 30-60 cps. range, and since lower values will cause rapid deterioration of the frequency response. Values of τ^2 and T will remain unspecified for the moment.

One of the most significant parameters in the performance of the system is velocity feedback in the major loop. Since system behavior changes most markedly with K_{vl}, the low frequency coefficient, this parameter was selected to show variation. The effects on the small-signal step response of changes in K_{vl} are shown in Fig. 4b.3. All responses are well within the specifications on rise time; but large K_{vl} induces excessive, unnecessary switching in the transient response, and small K_{vl} causes an underdamped response with possible overshoot. (It is easy to see from the responses with large K_{vl} why lead compensation was inserted.) The variation of the small signal frequency response with K_{vl} is shown graphically in Fig. 4b.4. Here it can be seen that this coefficient is critical in preventing peaking, although large values will cause a rapid deterioration of the frequency response.

Another parameter critical to system performance is K_F, the filter spring constant. Figure 4b.5 shows the differences in step response as K_F is changed. This variation is quite similar to that shown in Fig. 4b.3, which verifies that the product $\omega_n K_v$ sets the switching line. Differences in frequency response with changing K_F are shown graphically in Fig. 4b.6. As expected, for small values of K_F, the system bandwidth is reduced; however, we note that as K_F is increased above 1 in.-lb./rad. the low frequency portion (less than

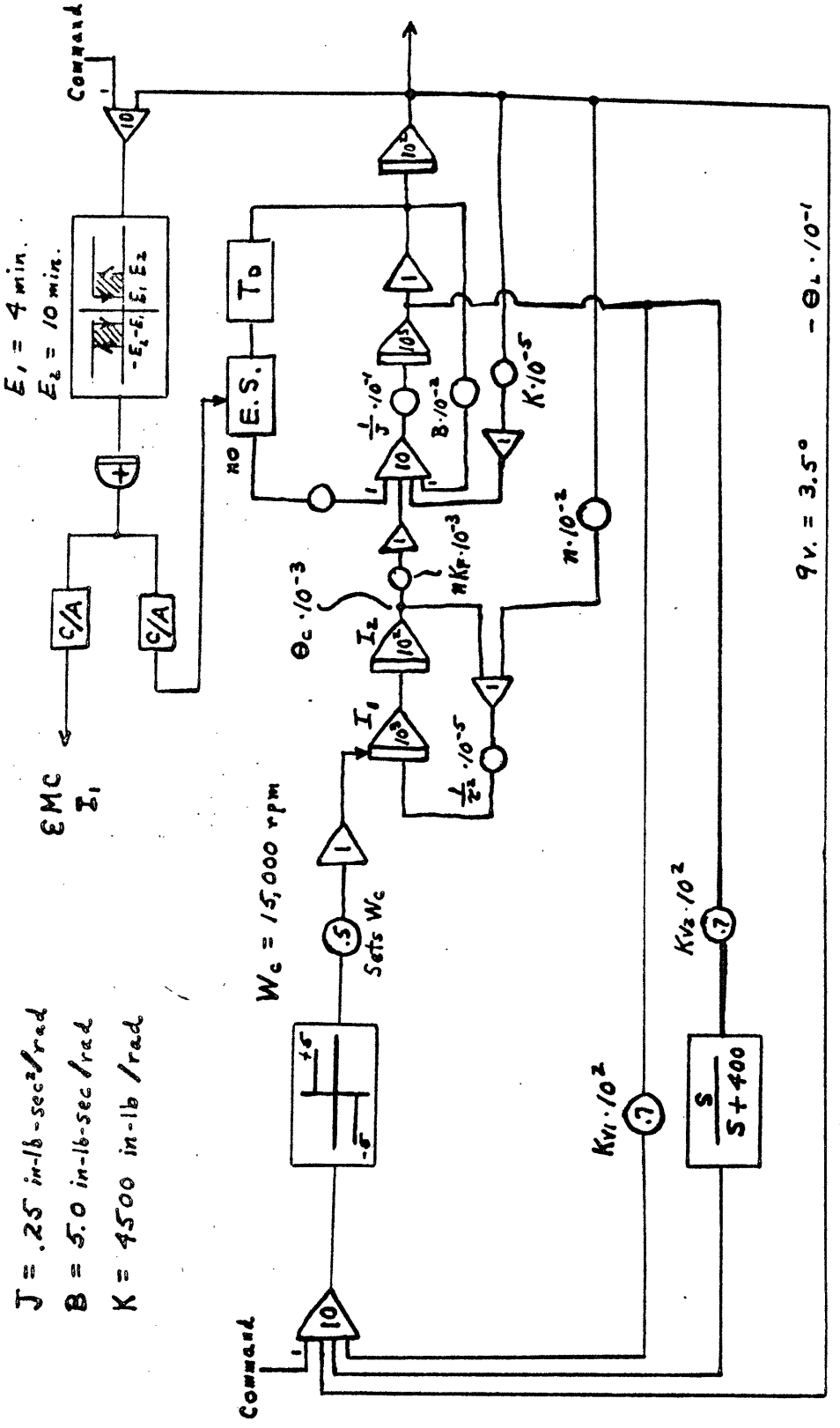

Fig. 4b.1 Analog Simulation Diagram for the Fixed-Point System of Chapter IV

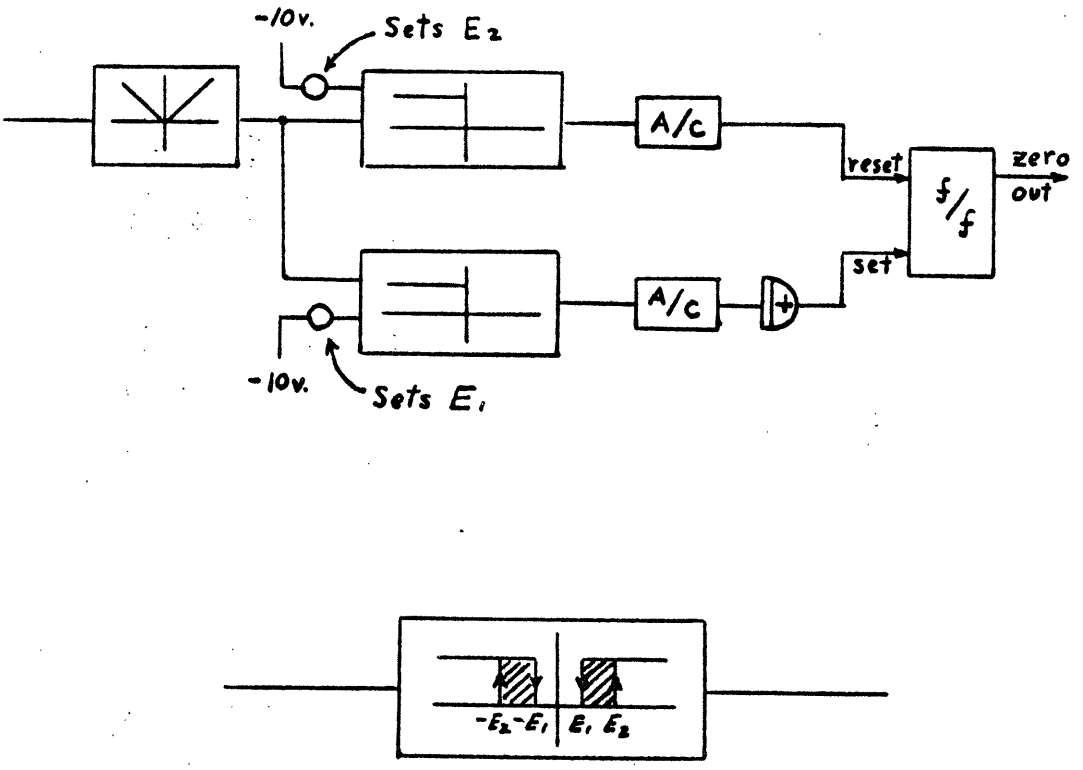

Fig. 4b.2 Analog Simulation and Block Symbol of the Hysteresis Device

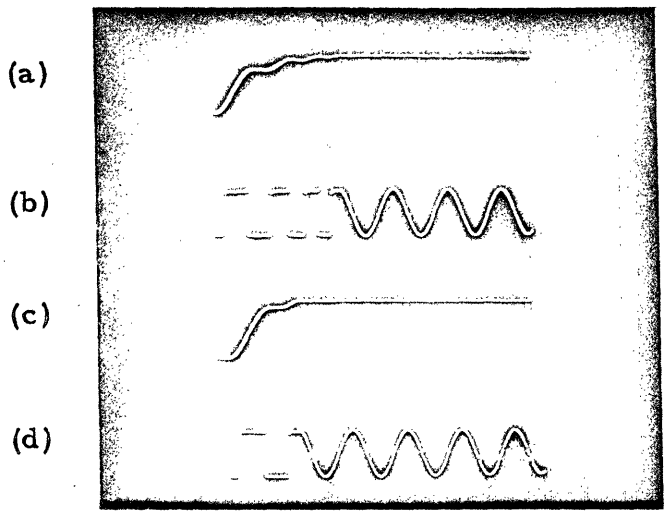

(a) Kv_1 = .008 sec.

(b) Switching waveform ($-\dot{\theta}_c$) for (a).

(c) Kv_1 = .007 sec.

(d) Switching waveform for (c).

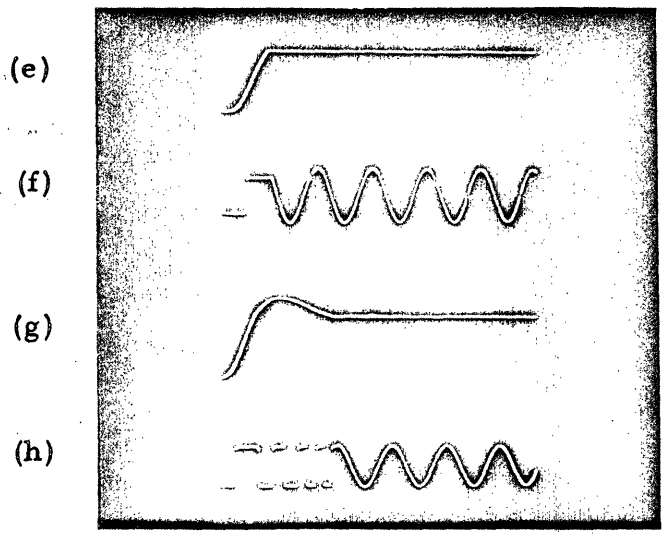

(e) Kv_1 = .006 sec.

(f) Switching waveform for (e).

(g) Kv_1 = .002 sec.

(h) Switching waveform for (g).

Duration of all traces = 100 msec.

Fig. 4b.3 Variation of Small-Signal Step Response with K_{v1}

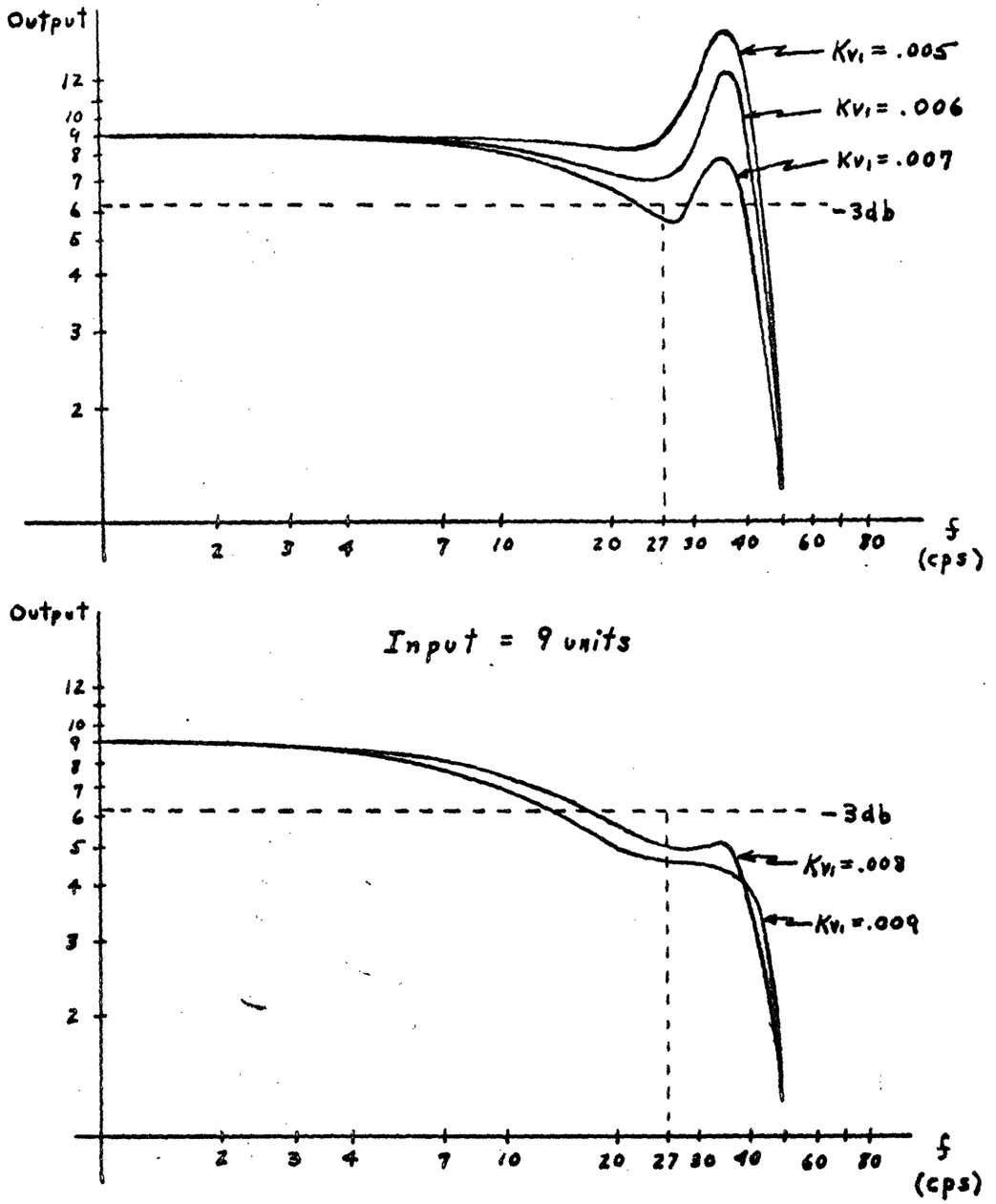

Fig. 4b.4 Variation of Small-Signal Frequency Response with K_{v1}

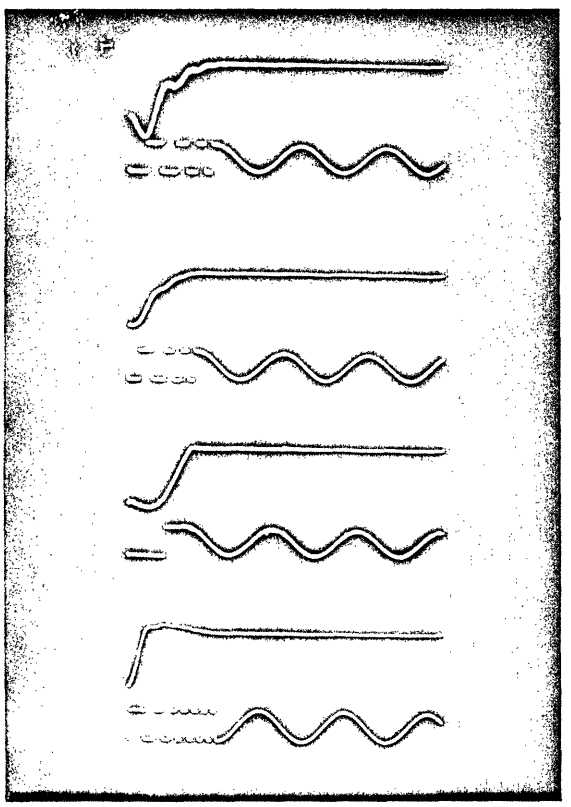

(a) K_F = 5.0 in-lb/rad.

(b) Switching Waveform ($-\dot{\theta}_c$) for (a)

(c) K_F = 3.0 in-lb/rad.

(d) Switching Waveform for (c)

(e) K_F = .50 in-lb/rad.

(f) Switching Waveform for (e)

(g) K_F = .25 in-lb/rad.

(h) Switching Waveform for (f)

Duration of all Traces = 100 msec.

Fig. 4b.5 Variation of Small-Signal Step Response with K_F

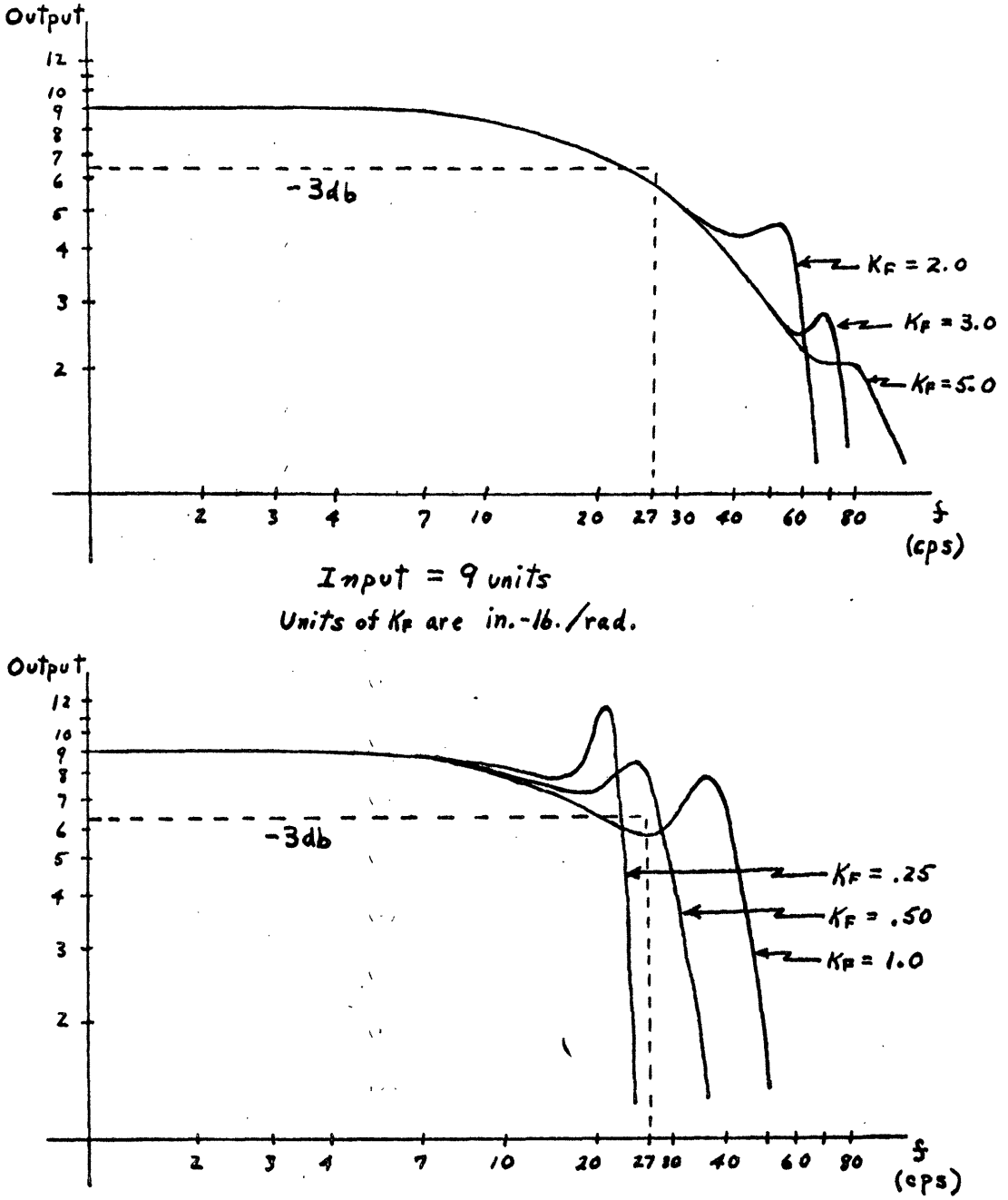

Fig. 4b.6 Variation of Small-Signal Frequency Response with K_F

30 cps) of the curve remains essentially unchanged. This probably reflects a basic limitation on speed of response due to the speed of the driving discs.

The last critical parameter to be varied is the speed of the driving discs W_c. Variation of the small signal step response is shown in Fig. 4b.7, and again the change in response is quite similar to Fig.4b.3. The small-signal frequency response with different values of W_c is shown in Fig. 4b.8, where an interesting phenomenon may be observed. As expected, for very low W_c the frequency response decays quite rapidly; however, as W_c increases from 7,500 rpm upward, the bandwidth actually decreases slightly with increasing W_c. This somewhat unexpected behavior reflects the fact that increasing the speed of the driving discs decreases high frequency peaking, (since the system is able to respond faster) and causes whatever peaking does exist to occur at higher frequencies. This behavior means that no resonance effects are in evidence in the 20-30 cps range, and consequently the response is down slightly compared with that of lower W_c. One should not infer from this, however, that an increase in W_c is to be avoided. As is shown in Fig. 3d.4, when peaking occurs the response can be quite far from sinusoidal, and thus a slight reduction in bandwidth may be preferable to having this peaking occur at low frequencies. Furthermore, an increase in W_c coupled with changes in other parameters may improve performance. This will be attempted shortly.

The data we have here should give us sufficient information for performing the optimization; however, some comments are in order with respect to other parameters. The values given for E_1 and E_2 appear to be good choices. Decreasing E_1 further causes noise problems (in the analog computer, at least) and experimentally proves to be of little advantage. E_2 need not be increased further since the system settles nicely into the dead zone with the present value, but decreasing E_2 would only defeat the purpose of the hysteresis. Typical steady state error in the step response with these values of E_1 and E_2 was found to be about 5 min., with 7 min. the maximum error. Actually, the system performance did not noticeably change because of the hysteresis device except that noise problems were

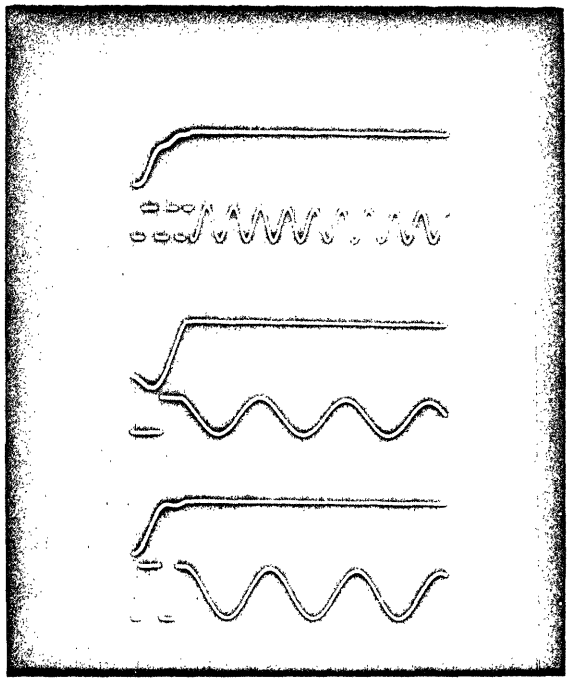

(a) 30,000 rpm < W_c < 60,000 rpm

(b) Switching Waveform ($-\dot{\theta}_c$) for (a)

(c) 3,000 rpm < W_c < 6,000 rpm

(d) Switching Waveform for (c)

(e) 10,000 rpm < W_c < 20,000 rpm

(f) Switching Waveform for (e)

Duration of all traces = 100 msec.

Fig. 4b.7 Variation of Small-Signal Step Response with W_c

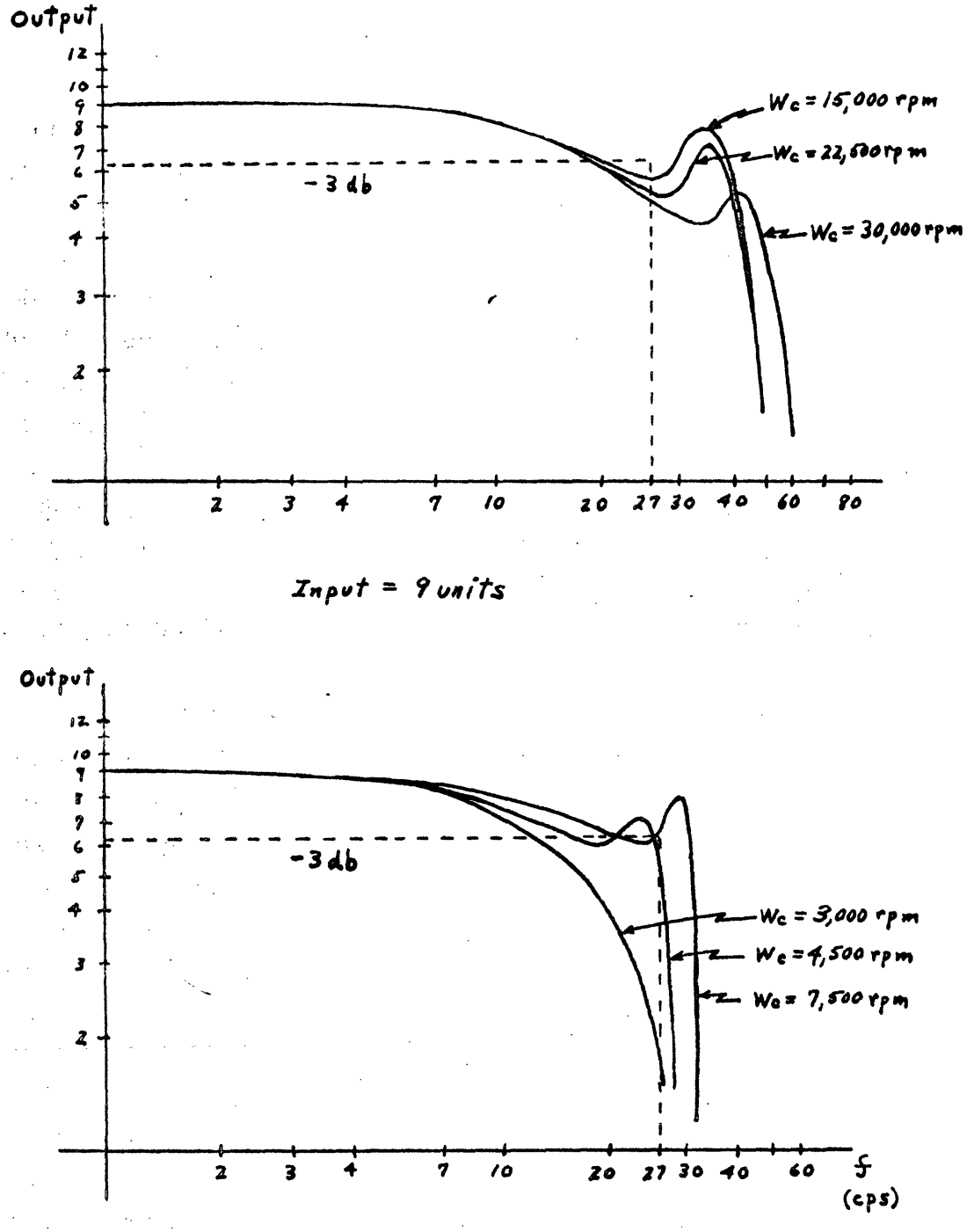

Fig. 4b.8 Variation of Small-Signal Frequency Response with W_c

greatly diminished. Drift in the analog computer was a significant problem, and the hysteresis device was a great help in keeping the system in the dead zone, for otherwise the step response would halt just within the edge of the dead zone and would quickly drift out. If noise is a major problem in the actual system, the hysteresis device may be of some use.

The value of J_F, the filter inertia, as was shown previously, should be made as small as possible, and there is therefore little to be gained from showing variations over this quantity. Optimization of this parameter is dictated only by physical constraints. This is also true for the gear ratio n, since to decrease n significantly could violate torque constraints, and as we saw previously, increasing n is of no help. The performance of the system does not depend noticeably on the value of T, the brake torque constant, as long as it is above a certain value. This minimum value was determined to be approximately 1000 in.-lb.

The only remaining parameter of interest is τ^2, which was defined previously as $\tau^2=J_c/K_F$. Clearly τ^2 should be made as small as possible, since, for a given value of W_c, the oscillations of J_c in mode 2 (see, for example, Fig. 4b.7) will be smaller in magnitude as J_c decreases. The major problem, of course, is that when the system switches from mode 2 to mode 1 the driven disc represented by J_c may be far out of position due to the oscillations, causing some rather wild transient responses for large τ^2. The system will recover more rapidly with large W_c, but for W_c in the range we have assumed, it was found that τ^2 should be less than 10^{-4} sec^2. For K_F=1.0 in.-lb/rad., this implies a value for J_c of less than or equal to 0.1×10^{-3} in.-lb.-$sec.^2$/rad., which appears reasonable. It should be mentioned that in the system model derived in Chapter II, there is assumed to be no friction in the clutch itself so that the simulated oscillations of J_c take several seconds to decay appreciably. In the actual system, however, friction in the clutch shaft should cause a sufficiently rapid decay of these oscillations to permit larger values of τ^2.

4c. The Optimum System

It can be seen from Figs. 4b.3 and 4b.4 that the system with the fixed-point parameter values of Section 4b comes very close to meeting all performance specifications. Reducing K_{v1} to .006 allows the one unsatisfied requirement (bandwidth) to be met, but only at a cost of increased peaking of the frequency response and underdamping of the step response. There is nothing to indicate, however, that the bandwidth specification cannot be satisfied without deterioration of other performance measures, and thus further investigation seems to be in order. Several areas are open for improvement, and these were investigated in the experimental work described next. In this work simultaneous variation of two or more parameters was explored as a means of improving performance.

The first approach attempted was a tradeoff between the high frequency component and the constant component of the velocity feedback. It seems likely that if more of the feedback is concentrated in the high frequency portion, system bandwidth may be increased with no increase in high frequency peaking. As a first measure, an increase in the high frequency breakpoint was attempted alone, but this proved to be unsuccessful in that increasing the breakpoint sufficiently to meet the 27 cps specification increased peaking to well above that of the fixed-point system. Reduction of K_{v1} along with an increase of K_{v2} was attempted in the hope of concentrating more damping in the high frequency portion, but again peaking increased for all values of the breakpoint equal to or greater than that of the fixed-point system. With the same type of tradeoff between K_{v1} and K_{v2} a decrease of the breakpoint was attempted, and this method offered some measure of success with the breakpoint near 300 rad./sec. It was found, however, that with the compensation becoming effective at such a low frequency, the frequency response waveforms became rough and nonsinusoidal even at low frequencies. Furthermore, switching in the step response was so slow that the response was effectively underdamped. Consequently further approaches were sought.

Experimentally it was observed that the most significant factor in determining the bandwidth of the system is the velocity feedback. If the frequency response is down at some given frequency, increasing

W_c or K_F does not increase the magnitude of the response unless the velocity feedback is decreased. Nevertheless, from Figs. 4b.6 and 4b.8 it appears that increasing W_c or K_F will eliminate peaking so that velocity feedback may be decreased without harm. Increasing W_c or K_F separately with reductions and tradeoffs in K_{v1} and K_{v2} was attempted, but this proved ineffective as peaking again increased and switching was destroyed in the step response. A very large increase in W_c (by a factor of ten, for example) did enable the bandwidth specification to be met, but in the range assumed for W_c the attempts were not successful. A similarly large reduction in W_c also decreases peaking by slowing the response (see Fig. 4b.8), but again lowering K_{v1} or K_{v2} sufficiently to meet the -3 db specifications increased peaking prohibitively.

In short, velocity feedback somehow must be decreased, but coupling this reduction with change of another single parameter is not successful. The only remaining approach is to reduce the velocity feedback in some way and to increase both W_c and K_F. It is unfortunate, of course, that both K_F and W_c have to be increased, but it is nonetheless fortunate that this one remaining method did prove to be successful in improving performance. The proposed optimum system was obtained by decreasing K_{v1} to .006 and increasing K_{v2} to .010 while increasing the breakpoint to 700 rad./sec. W_c was increased to 20,000 rpm, and K_F had to be increased to 2.0 in.-lb./rad. All else in the optimum system was not changed from the fixed-point values of Section 4b.

The final schematic of the optimum system is shown in Fig. 4c.1, and the accompanying block diagram is shown in Fig. 4c.2. In both figures the velocity feedback compensation has been recombined to form a lead network according to Eq. 4a.1. The corresponding performance of the optimum system is demonstrated in Figs. 4c.3, 4c.4, and 4c.5, and it may be noted that all specifications are satisfied. The pertinent data of the optimum system are as follows:

Filter Spring Constant: $K_F = 2.0$ in.-lb./rad.

Filter Inertia: $J_F = .08 \times 10^{-3}$ in.-lb.-sec.^{2}/rad.

Tachometer Coefficient: $K_v = .016$ sec.

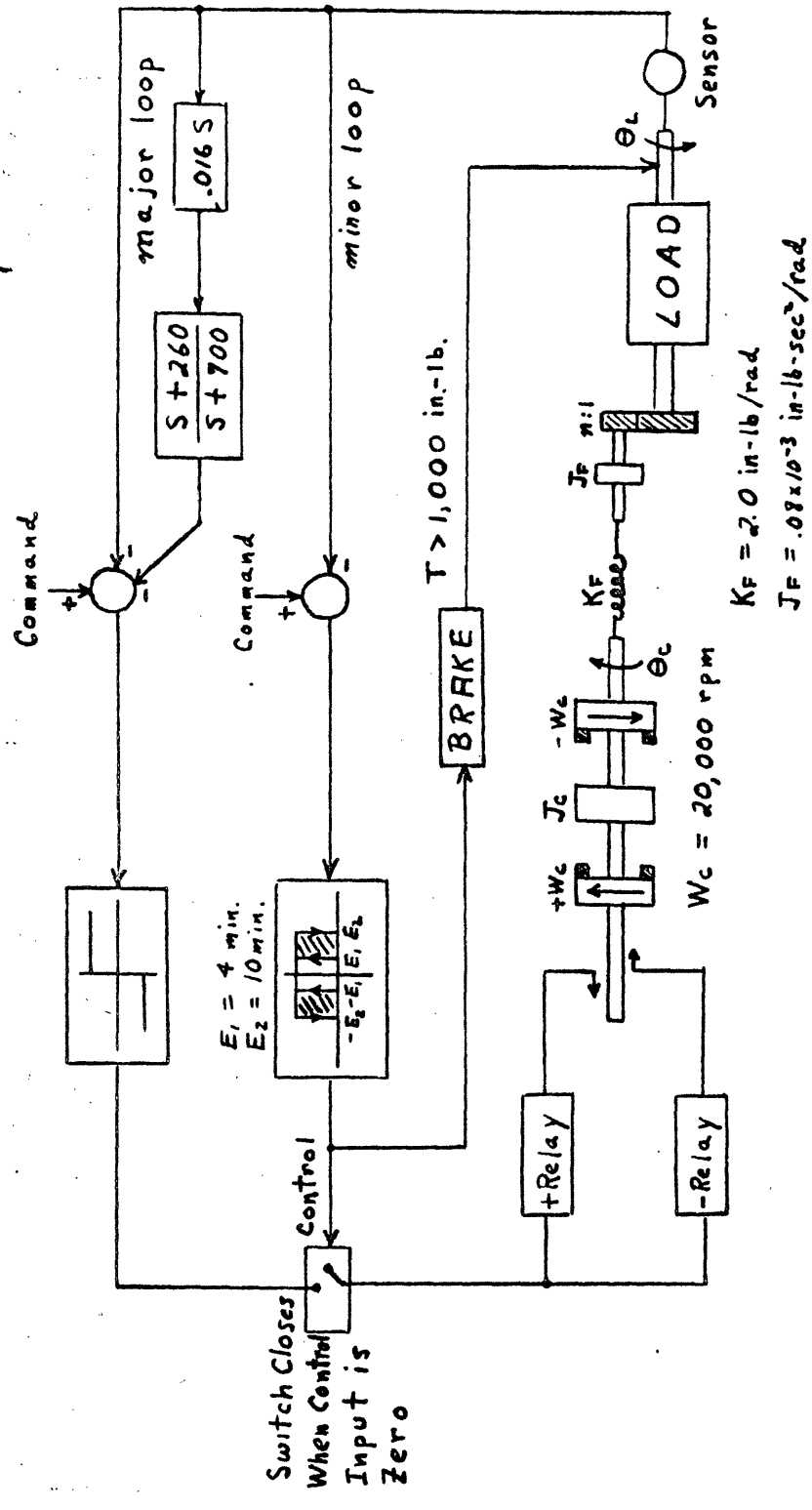

Fig. 4c.1 Schematic Diagram of the Optimum System

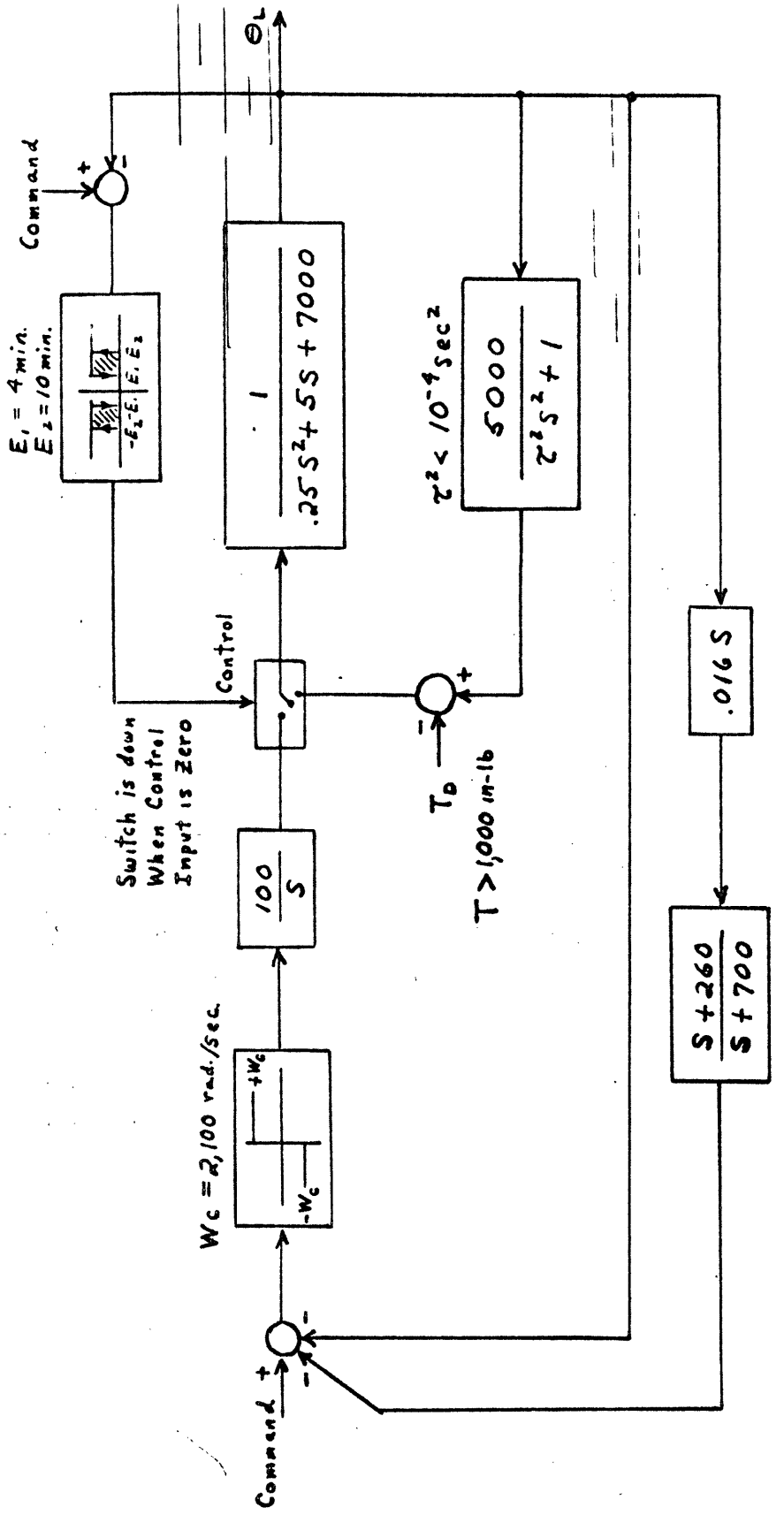

Fig. 4c.2 Block Diagram of the Optimum System

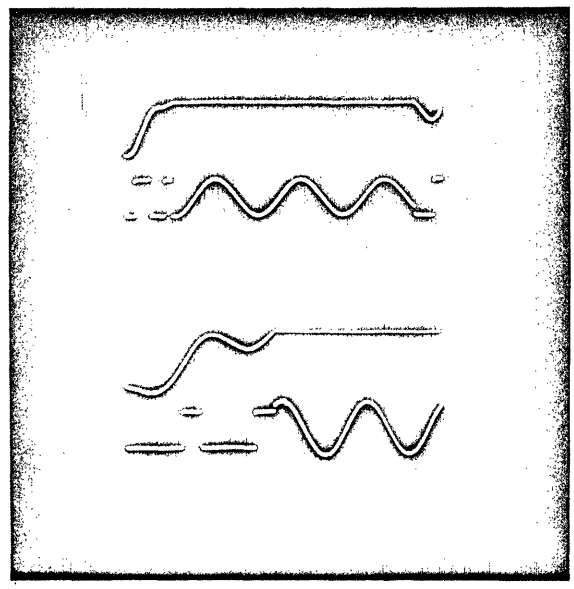

(a) Small-Signal Step Response.
Duration of Trace = 100 msec.

(b) Switching Waveform ($-\dot{\theta}_c$) for (a)

(c) Large Signal (30^o) Step Response
Duration of Trace = 100 msec.

(d) Switching Waveform for (c)

Steady State Error less than 7 minutes.

Fig. 4c. 3 Step Response of the Optimum System

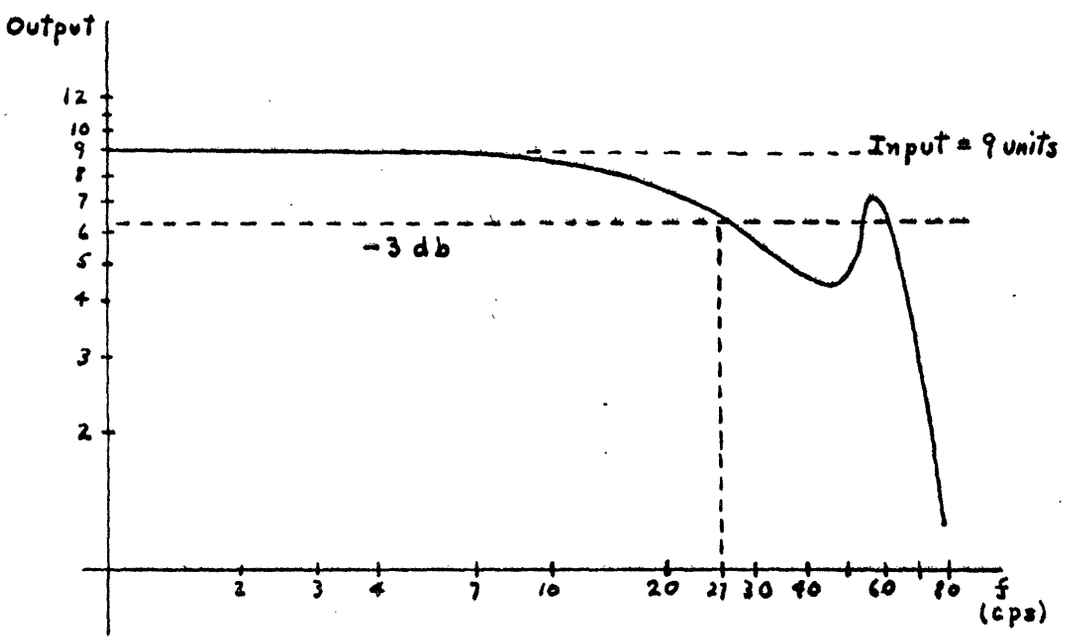

Fig. 4c.4 Small-Signal Frequency Response of the Optimum System

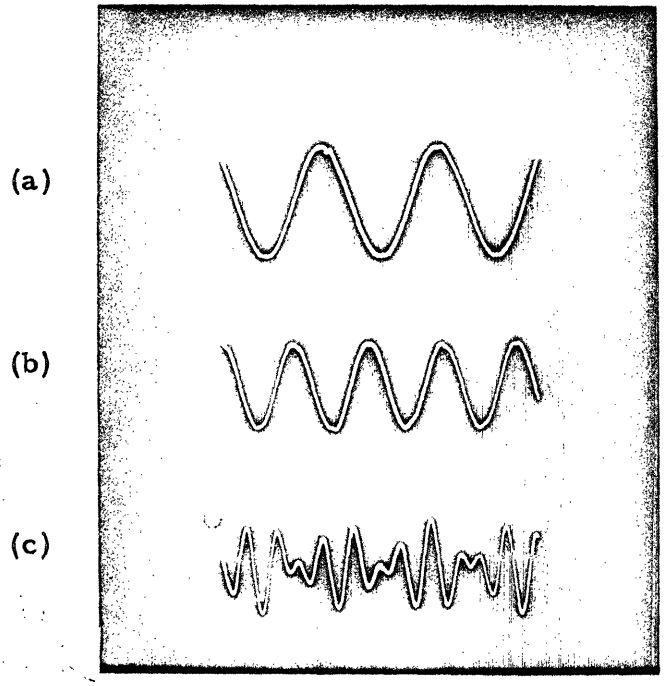

(a) 5 cps.

(b) 20 cps.

(c) 55 cps.

Fig. 4c.5 Small Signal Sinusoidal Response Waveforms for the Optimum System

Tachometric Compensation: $\frac{s + 260}{s + 700}$

Gear Ratio: $n = 50$

Speed of Driving Discs: $W_c = 20,000$ rpm

Break Torque Constant: $T > 1,000$ in.-lb.

Clutch Inertia: $J_c < 0.2 \times 10^{-3}$ in.-lb.-sec.^{2}/rad.

Natural Frequency of the Linear Subsystem: $\omega_n = 167$ rad./sec. $= 27$ cps

Damping Ratio of the Linear Subsystem: $\zeta = .06$

Typical Small Signal Rise Time: 20 msec.

Typical Steady State Error: 5-7 min.

Width of Inner Dead Zone: $E_1 = 4$ min.

Width of Outer Dead Zone: $E_2 = 10$ min.

4d. Preliminary Conclusions

The optimum system proposed in Section 4b meets all of the performance specifications given in Chapter I. Furthermore, all parameter values seem to represent physically realizable quantities, and switching seems to have been kept to a reasonably low level. Thus there appears to be no reason why a system could not be realized which fulfills all the objectives stated in Chapter I. It must be recalled, however, that these conclusions are based on the rather simple system model derived in Chapter II, in which the effects of delay and slippage are neglected. Final conclusions must be left to Chapter V where the effects of delay are accounted for.

CHAPTER V

FURTHER INVESTIGATION AND FINAL CONCLUSIONS

In this chapter the system model derived in Chapter II will be improved slightly by consideration of delay in switching. An investigation also will be made into whether tachometric feedback can be avoided without loss of performance. Final conclusions will be given.

5a. Effects of Delay in Switching

In all previous work we have adhered to the assumption made in Chapter II that when the clutch is engaged, its shaft immediately assumes velocity $\pm W_c$. In reality, of course, there must be a finite delay between the time a switch is indicated and the instant that the shaft arrives at velocity $\pm W_c$. This delay will be the result of the combined effects of delay in energizing the relays and of delay due to slippage in the clutch. Since it would be difficult, if not impossible, to estimate the magnitude of this delay time with no mechanical knowledge of the clutch, we will instead observe the effects of various delay times on system performance. In the following work we will assume that both slippage and relay delay may be accounted for by a pure time delay. Although this is clearly not the case, it can be seen that the assumption represents a conservative rather than a helpful estimate.

Thus to include the effects of switching delay in the block diagram of the optimum system (Fig. 4c.2), we need only insert a delay block after the two-state element in the major loop. We will find that due to the delay the system will not switch quickly enough unless proper compensation is employed and the velocity feedback is increased. Experimentally it is found that the previously employed lead compensation of the velocity feedback is sufficient in this respect, and thus the block diagram of the optimum system need only be modified slightly to the form shown in Fig. 5a.1. No attempt will be made to optimize the system repeatedly as the delay is increased, and thus the performance obtained may not be the best attainable. The only changes which will be made will be in the velocity feedback loop.

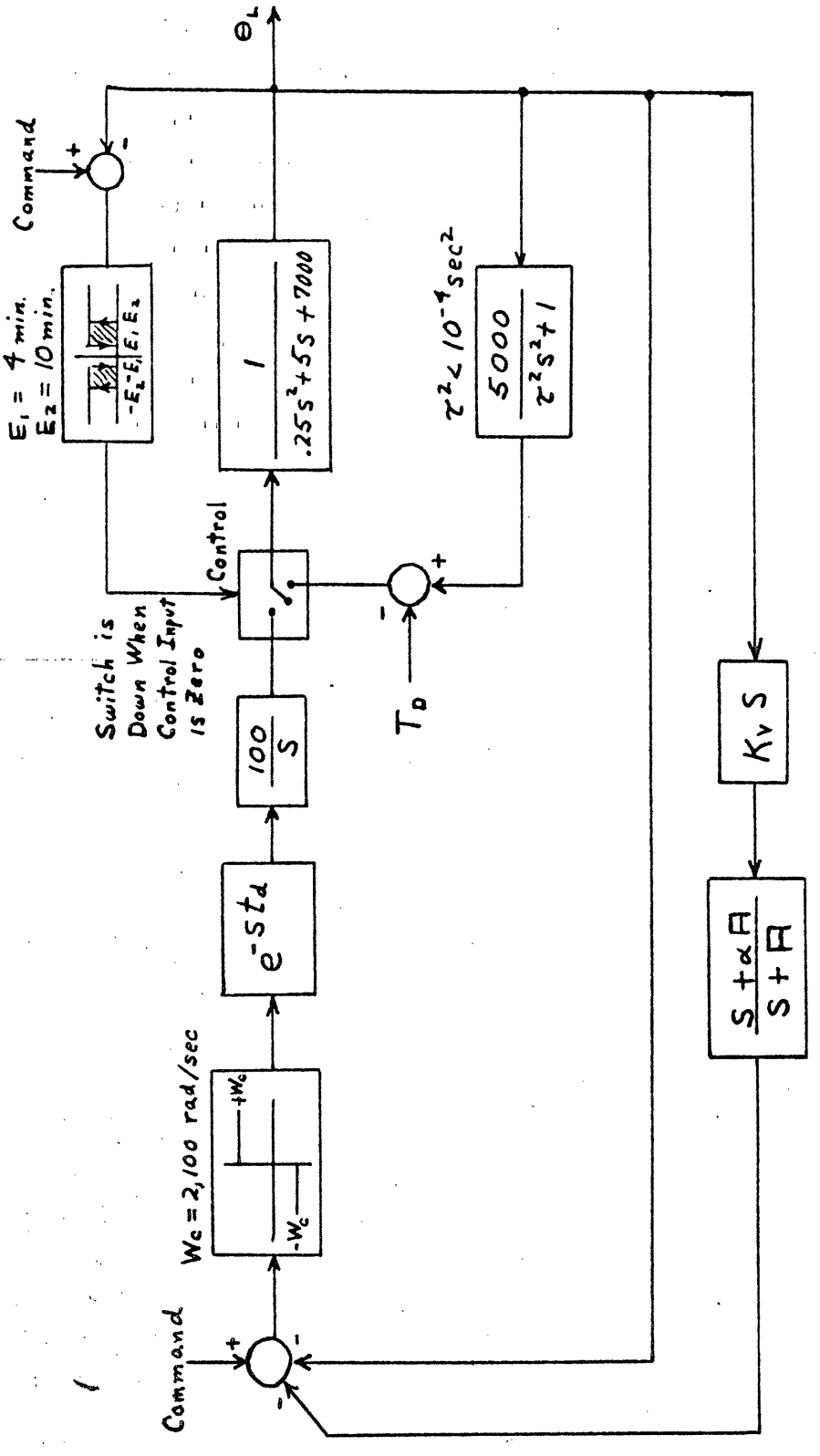

Fig. 5a.1 Block Diagram of the Optimum System with Delay

The simulation diagram for the system with delay need not be presented here since it requires only a slight modification of Fig. 4b.1; however, the means of simulating the delay does require some explanation. The method used by Firodia will be employed here because of its simplicity and applicability to the specific waveform being delayed. A block diagram of the delay network is given in Fig. 5a.2 along with some waveforms indicating the behavior of the network. The output of the two-state element is fed into a first order lag network with transfer function $\frac{1}{1+sT_1}$, and the output of the lag network is in turn fed into a hysteresis element. The output of the hysteresis device is a train of rectangular pulses which lag those of the two-state device by a preset delay time, t_d, the value of which may be adjusted by varying T_1. Figure 5a.3 shows the simulation diagram for this time delay network.

The variation of system performance will be shown for delays of 0.5 msec., 1.0 msec., and 1.5 msec. As the delay assumes these values, the compensation network and the coefficient K_v will be varied as shown in Table 5a.1. K_v must be increased with increasing

Table 5a.1

Compensation Network and Feedback Coefficient for Various Delay Times

Delay, t_d	K_v	Compensation, $\frac{s+\alpha A}{s+A}$
0	.016 sec.	$\frac{s+260}{s+700}$
0.5 msec.	.025 sec.	$\frac{s+500}{s+700}$
1.0 msec.	.050 sec.	$\frac{s+900}{s+1000}$
1.5 msec.	.060 sec.	$\frac{s+900}{s+1000}$

delay in order to maintain transient switching and to prevent peaking of the frequency response. The form of the lead network is set mainly by the frequency response, as this compensation acts to smooth the output waveforms by increasing the frequency of switching. This compensation performs a similar smoothing function for transient

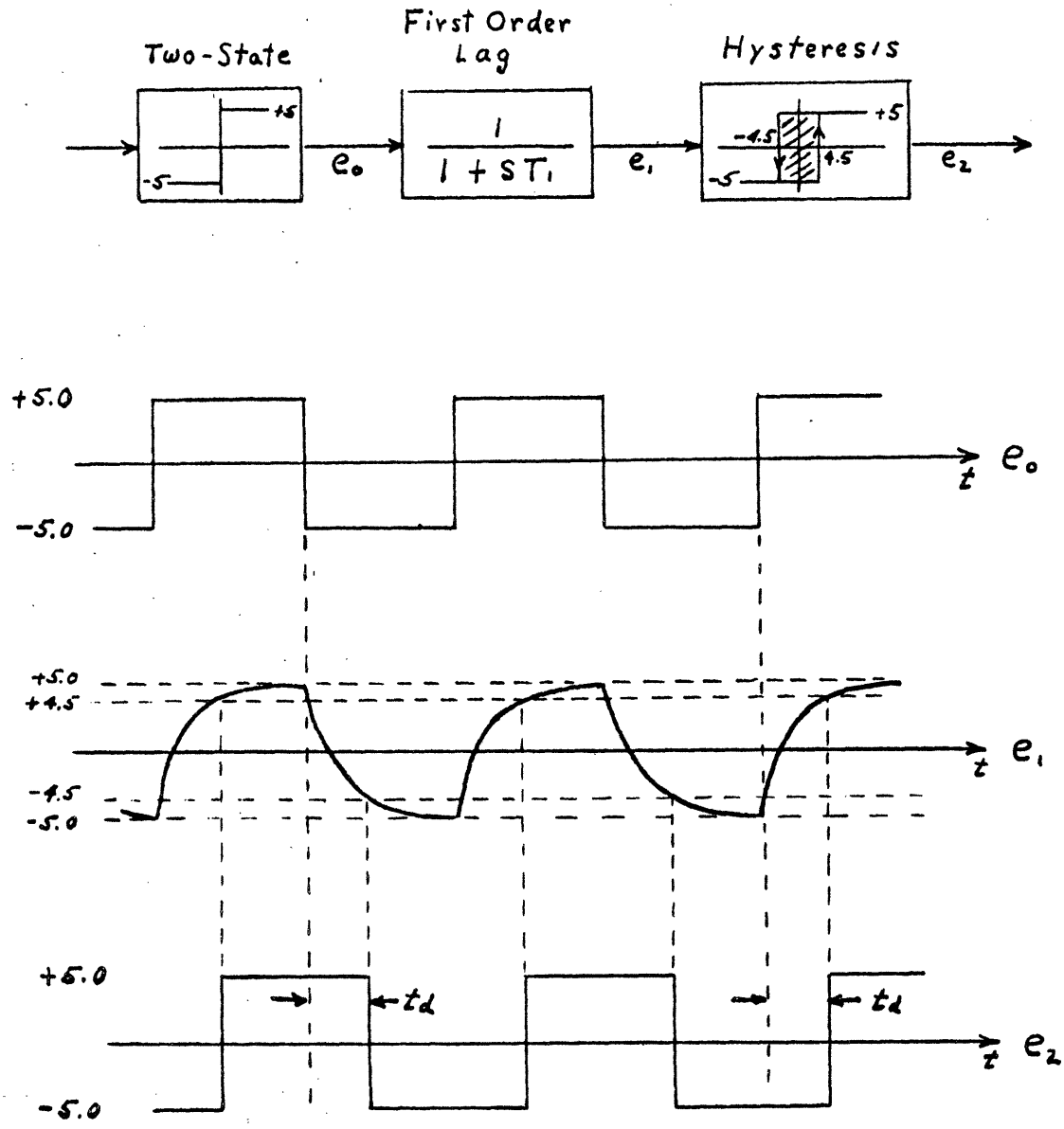

Fig. 5a.2 Time Delay Network

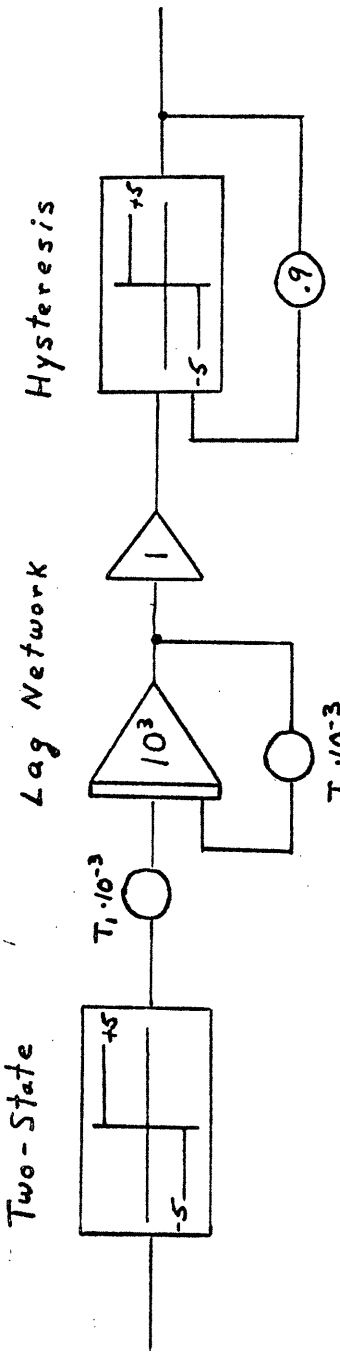

Fig. 5a.3 Analog Simulation of the Time Delay

responses by making the transient switching faster, although not more frequent. The form of the lead network becomes critical to the frequency response as delay increases, since too little lead (i.e., α of Table 5a.1 too large) causes excessive peaking, and too much lead results in slow switching and very rapid decay of the frequency response. It seems justified to assert that the form of this compensation can only be determined experimentally.

The effects of delay on the small signal step response are shown in Fig. 5a.4, and the changes in the small signal frequency response are shown graphically in Fig. 5a.5. It may be noted that specifications on the rise time are still easily satisfied, and in all cases the step response remains reasonably well damped. In addition, reduction of bandwidth is appreciable only for t_d=1.5 msec, for which the -3 db point occurs near 23 cps. This is to be expected, however, since increasing delay places an unavoidable upper limit on the speed of response of the system.

Peaking is generally decreased when delay is present, and this seems to suggest a decrease in velocity feedback to increase bandwidth. K_v could not be decreased, however, since this was found to destroy switching in the step response. A final observation may be made, from a comparison of Figs. 5a.6 and 4c.5, that increasing delay is somewhat detrimental to the frequency response waveforms. Nevertheless, it is evident that the general results of Chapter IV have not been invalidated by the introduction of delay into the system model, and it is clear that all specifications will continue to be met if the delay is sufficiently small.

5b. A System Without Velocity Feedback

As was mentioned in Chapter I, in the interests of economy and simplicity it is desirable to avoid velocity feedback if possible. To determine whether this can be done, a system was investigated which employs compensation of the position feedback in place of velocity feedback. (Except for this change the optimum system with no delay will be used in this section.) The compensation may be of the form 1+F(s), where F(0)=0 since steady state error must be fed unchanged to the two-state device. A logical and convenient choice for F(s) is

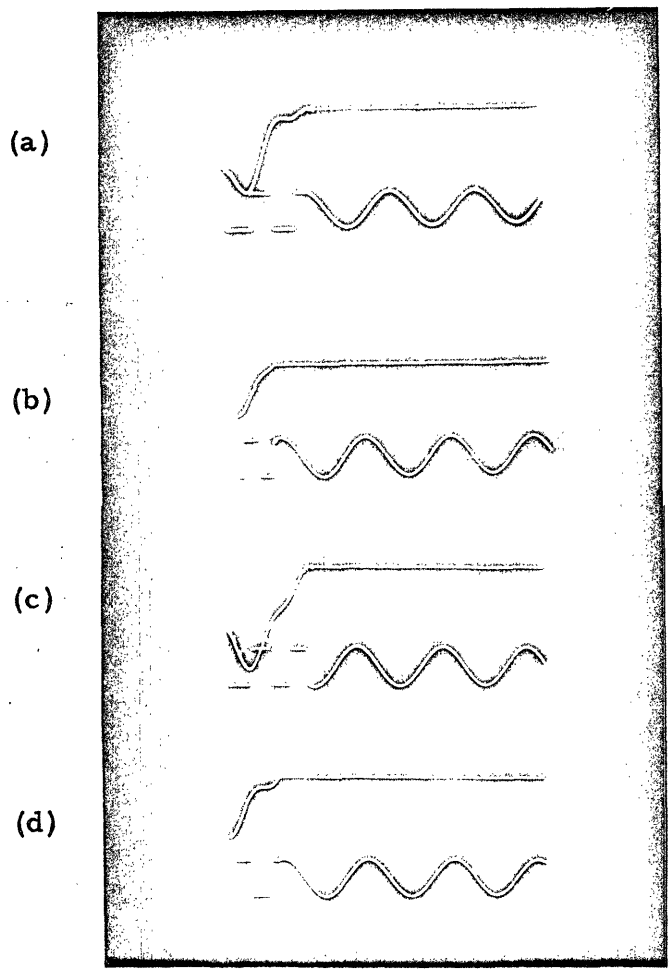

(a) Delay = 0.5 msec.

(b) Delay = 1.0 msec.

(c) Delay = 1.5 msec.

(d) Delay = 1.5 msec.

Duration of all Traces = 100 msec.

Fig. 5a.4 Effects of Switching Delay on the Small-Signal Step Response

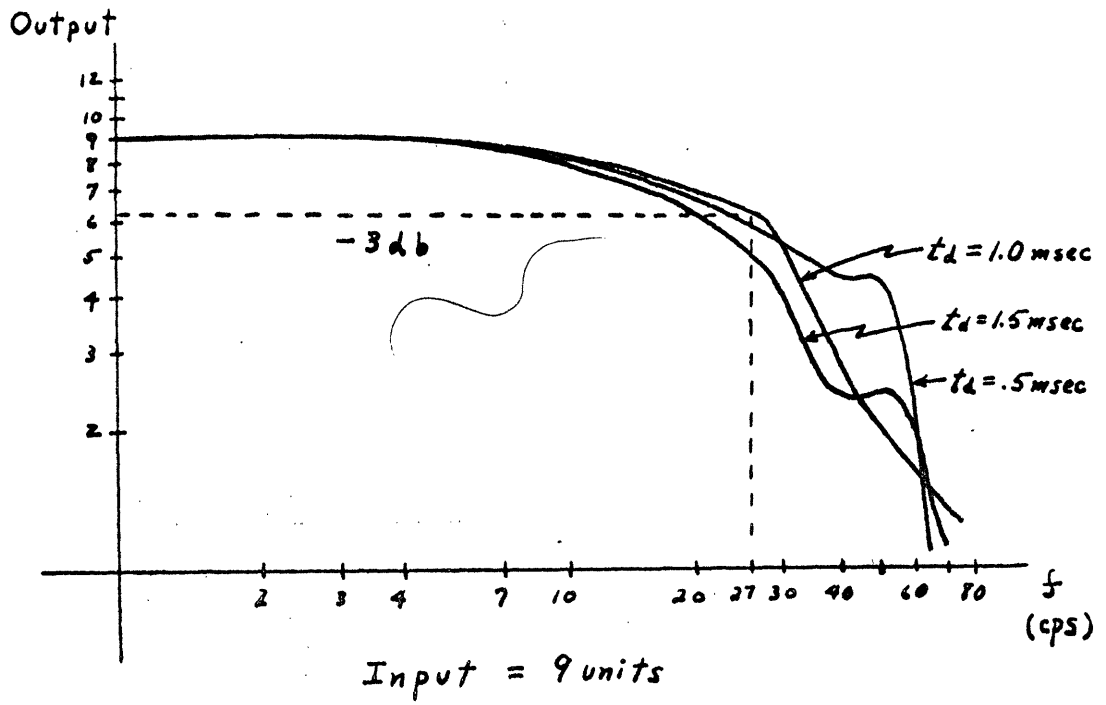

Fig. 5a.5 Effects of Switching Delay on the Small-Signal Frequency Response

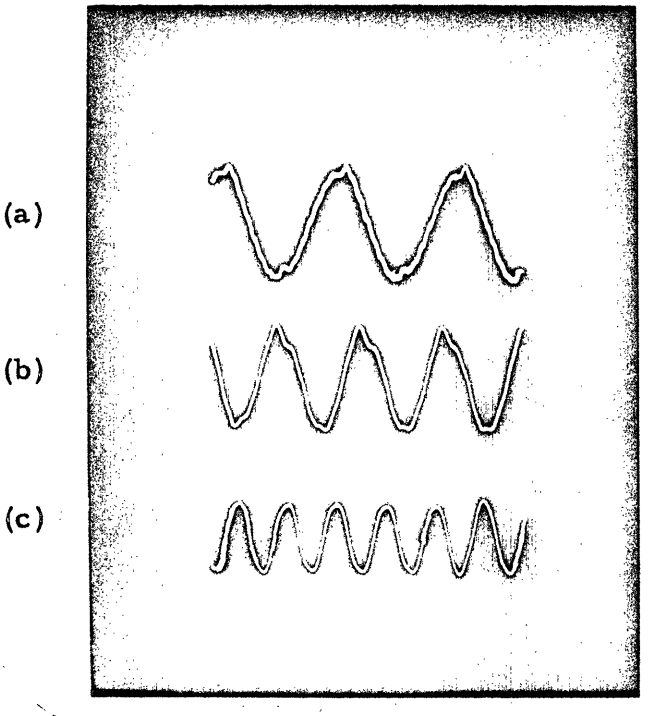

(a) 7 cps

(b) 15 cps

(c) 30 cps

Fig. 5a.6 Some Small-Signal Sinusoidal Response Waveforms for Delay = 1.0 msec.

$K_c \frac{s}{s+B}$, and the results obtained previously seem to suggest this type of compensation. If K_c is made sufficiently large, reverse switching should be induced in the transient response, and high frequency damping should be provided.

The data of Chapter IV seem to indicate that if $K_v=0$, then W_c should be reduced significantly if excessive peaking (or even instability) is to be avoided. This indeed proved to be the case, as no values of K_c and B could be found to give a stable step response for W_c larger than 3,000 rpm. Instability of this system is almost certain if overshoot occurs in the step response, and for W_c above 3,000 rpm no values of K_c and B could be found to induce reverse switching and prevent overshoot. For W_c between 1,500 and 3,000 rpm the step response becomes stable; but peak magnification of the frequency response is always greater than 1.4 for any form of the compensation, and instability of the frequency response is a possibility.

Only for W_c less than 1,000 rpm is significant reverse switching possible in the step response; but when this switching is induced, the frequency response is not flat out to 7 cps and the -3 db point occurs lower than 20 cps. For W_c less than 1,500 rpm but large enough to satisfy the 7 cps specification, peak magnification of the frequency response is always greater than 1.4, and the corresponding peaking generally occurs at frequencies less than 20 cps. In addition, the -3 db point occurs in the range 22-24 cps, and the response is down about 6 db at 27 cps.

In summary, it does not appear that specifications can even nearly be met with the system described in this section. Velocity feedback has the effect of stabilizing the system, and it appears that reliable performance is not possible without it. In a nonlinear system instability is always possible as a result of an anamalous input, but the system with velocity feedback seems much more likely to recover from such an input than does the system of this section.

5c. Final Conclusions and Recommendations

Within the accuracy of the mathematical model it has been found possible to design a three-state clutch servomechanism which

fulfills all of the specified objectives. If the clutch is used in the two-loop control system presented in Chapter III, the optimum system of Chapter IV is able to meet all the proposed performance specifications. The parameter values of this optimum system appear to be physically reasonable and do not seem to prohibit an actual realization of the system. Switching in the clutch has been held to a reasonably low level, and thus delay in switching does not cause a drastic deterioration in performance. As verified in Chapter V, only bandwidth requirements become a problem as delay is increased up to 1.5 msec. Thus the switching speed of the clutch and its susceptibility to slippage may cause limitations in bandwidth, but aside from this reservation, all objectives have been met.

The results of the simulation studies seem to recommend that steps toward a physical realization of the system be undertaken, but as mentioned earlier, these results must be evaluated in light of mechanical constraints. The switching delay in the clutches (including the effective delay due to slippage) probably should not be greater than 1.5 msec., and it may not be possible to find such a clutch with an adequate torque rating. The clutch must be capable of switching 3 to 4 times in 15 msec. (see the small signal step response) and this rate may be unrealistic or may lead to excessive heating. Heat dissipation may also be significant in the brake, although this does not appear to be the case in the simulations. (Quantitative results were not obtained.) All these factors should be investigated before a physical realization is attempted.

Finally, there is one other point which may require investigation. We have assumed throughout our work that system parameters are constant, but in reality external factors, such as vehicle velocity, may influence parameter values. The exact value of K_L is not critical because of the filter spring; but B_L and J_L are crucial to the system natural frequency and damping ratio. Thus large variations in B_L and J_L may not be tolerable. Research should be conducted to determine whether system performance will be radically affected by uncertainty or variation in these coefficients. (For example, is the damping ratio a major factor in system performance?) If all of the above investigations produce positive results, then a physical realization of the system should be made.

BIBLIOGRAPHY

1. Cheney, R. W., "A Nonlinear Clutch Servomechanism for Underwater Control Surface Actuation," MIT Thesis, Course XVIII, August, 1966.

2. Firodia, A. H., "A Nonlinear Clutch Servomechanism Employing Two-state Modulation," MIT Thesis, Course VI, February, 1967.

3. Thaler and Pastel, Analysis and Design of Nonlinear Feedback Control Systems, McGraw-Hill, 1962.

4. Villamizar, A. R., "Parameter Determination of Dry Magnetic-Particle Clutch in Switching Mode Operation," MIT Thesis, Course VI, August, 1966.

5. Specification for Electromechanical Actuator System, NUOS No. 3.27.65/ASP.